



Capillary electrophoresis for enzyme-based studies: Applications to lipases and kinases

Ghassan Al Hamoui Dit Banni, Reine Nehmé

► To cite this version:

Ghassan Al Hamoui Dit Banni, Reine Nehmé. Capillary electrophoresis for enzyme-based studies: Applications to lipases and kinases. *Journal of Chromatography A*, 2022, 1661, pp.462687. 10.1016/j.chroma.2021.462687 . hal-03706495

HAL Id: hal-03706495

<https://univ-orleans.hal.science/hal-03706495>

Submitted on 5 Jan 2024

HAL is a multi-disciplinary open access archive for the deposit and dissemination of scientific research documents, whether they are published or not. The documents may come from teaching and research institutions in France or abroad, or from public or private research centers.

L'archive ouverte pluridisciplinaire **HAL**, est destinée au dépôt et à la diffusion de documents scientifiques de niveau recherche, publiés ou non, émanant des établissements d'enseignement et de recherche français ou étrangers, des laboratoires publics ou privés.



Distributed under a Creative Commons Attribution - NonCommercial 4.0 International License

Capillary electrophoresis for enzyme-based studies: applications to lipases and kinases

Ghassan Al Hamoui Dit Banni and Reine Nehmé*

Institut de Chimie Organique et Analytique (ICOA), CNRS FR 2708 – UMR 7311, Université d'Orléans, 45067 Orléans, France

* reine.nehme@univ-orleans.fr

Abstract

Capillary electrophoresis (CE) is a powerful technique continuously expanding into new application fields. One of these applications involves the study of enzymes, their catalytic activities and the alteration of this activity by specific ligands. In this review, two model enzymes, lipases and kinases, will be used since they differ substantially in their modes of action, reaction requirements and applications making them perfect subjects to demonstrate the advantages and limitations of CE-based enzymatic assays. Indeed, the ability to run CE in various operation modes and hyphenation to different detectors is essential for lipase-based studies. Additionally, the low sample consumption provided by CE promotes it as a promising technique to assay human and viral nucleoside kinases. Undeniably, these are rarely commercially available enzymes and must be frequently produced in the laboratory, a process which requires special sets of skills. CE-based lipase and kinase reactions can be performed outside the capillary (pre-capillary) where the reactants are mixed in a vial prior to their separation or, inside the capillary (in-capillary) where the reactants are mixed before the electrophoretic analysis. These enzyme-based applications of CE will be compared to those of liquid chromatography-based applications in terms of advantages and limitations. Binding assays based on affinity CE and the compelling microscale thermophoresis (MST) will be briefly presented as they allow a broad understanding of the molecular mechanism behind ligand binding and of the resulting modulation in activity.

Keywords

Affinity assays, capillary electrophoresis, catalytic activity assays, kinases, lipases, microscale thermophoresis

33	Outline	
34	1. Introduction.....	3
35	2. CE-based lipase assays.....	5
36	3. CE-based nucleoside kinase assays.....	16
37	4. Conclusion.....	23
38	5. Declarations	23
39	6. References.....	24
40		

1. Introduction

Enzyme catalyzed reactions and abnormal perturbations in their function are implicated, either directly or indirectly, in the development of several disorders such as infections [1,2], cancers [3,4], obesity [5] or skin aging [6]. Assaying the catalytic activity of enzymes expedites the elaboration of the molecular mechanisms through which enzymes function and influence the development of diseases [7]. This often implicates the evaluation of kinetic parameters of the enzyme catalyzed reaction, such as: the maximal velocity (V_{\max}), the Michaelis-Menten constant (K_m) or the turnover number (K_{cat}).

Additionally, the activity of an enzyme can be measured in the presence of modulatory molecules that diminishes or enhances the enzyme's activity. This allows the evaluation of the degree of modulation upon comparison to the innate enzymatic reaction, *i.e.* in the absence of modulatory molecules. The half maximal inhibitory (IC_{50}) or activation (AC_{50}) concentrations are two parameters that can be used to rank activators and inhibitors in terms of their potency in modulating an enzyme's activity.

Another approach is to evaluate the equilibrium dissociation constant (K_d), or sometimes referred to as K_i . K_d allows the prediction of the binding affinities between potential substrates/ligands and target enzymes and is an important preliminary step for drug screening [8]. Both of these approaches facilitate, through their complementarity, the establishment of a structure - activity relationship (SAR) which can then act as a guideline for prioritizing certain ligands over others for their therapeutic use [9].

All of the aforementioned parameters of enzymatic activity, modulation and binding affinities and details will be revisited later on throughout this review. More details behind their conception and applications can be acquired from several previous sources [10–13].

In addition to being drug targets themselves, enzymes can be used in the pharmaceutical industry for the synthesis of active pharmaceutical compounds. Additionally, other industries such as the food, biofuels and chemical industries have adapted the use of enzymes in their line of production [14]. Some of the common examples for the implementation of enzymes in industrial processes may be the production of lactose free dairy through the use of lactase enzymes [15] or in the production of protease or lipase containing washing detergents [16].

For the last 10 years, various techniques have been reviewed and described for assaying enzymatic activities as well as screening for drug candidates [6,9,17–25]. There exists no “one technique to

rule them all". Enzymes have different physical and chemical requirements and therefore some assays may be unsuitable and must be modified or replaced. The choice of the technique depends on several factors such as the relevance of the collected information, the price of the reagents and the compatibility of the technique with the nature of the investigated enzymatic reaction [26].

Capillary electrophoresis (CE) is an analytical separative technique with applications in various fields including enzymatic analysis. The substrate(s) and product(s) are separated in an open capillary based on their charge-to-size ratio in an electric field applied across the capillary. Enzymatic analysis with CE is associated with several advantages such as low sample and reagent consumption, excellent separation efficiency and high versatility of hyphenation and operation modes [27]. CE-based enzymatic reactions can be divided into pre-capillary (offline) and in-capillary (online) reactions, where in the former, all the reagents, except one (substrate or enzyme), are incubated in a vial outside the capillary [28]. The reaction is initiated by adding the missing reagent (enzyme or substrate). Offline CE-assays are easy to optimize since the enzymatic reaction and analyte separation occur independently. Due to this division in tasks, these assays are easy to control. Manual interventions are, however, inevitable when handling reactions offline and relatively large reaction volumes are required (few tens of μLs) [28,29]. On the other hand, with the online CE reaction mode, the capillary acts as a nanoreactor in which the reaction, separation and detection steps take place. There exist several methodologies by which the reactants are mixed in-capillary such as electrophoretically mediated microanalysis (EMMA) [30,31] or transverse diffusion of laminar flow profiles (TDLFP) [32]. These types of assays are often difficult to optimize and to control due to the fact that all steps occur sequentially within the capillary. Nonetheless, online assays are considerably more automated compared to offline ones.

CE can also be expanded to measure macromolecular binding interactions through the use of affinity CE (ACE). This mode generally exploits the different electrophoretic mobilities of unbound and bound complexes for their separation and quantification and may be fine-tuned according to the application [33,34].

In terms of the overall performance, CE is often compared to the analytical technique widely used by laboratories around the world, liquid chromatography (LC). Unlike CE, separation of analytes in LC is based on their retention by a solid phase in a column. Although more commonly used for separation of mixtures between two immiscible phases, LC have also been used for enzymatic analysis [35].

Several recent papers have reviewed the state of the art of CE-based enzymatic analyses [36–38]. In this review, we go a step further by tracking the evolution, flexibility and adaptability of CE-based enzymatic analyses through the use of two enzyme models, lipases and nucleoside kinases. Both said enzymes have dissimilar modes of actions, reaction requirements and require different analysis approaches making them thus suitable models of simple and complex reactions to demonstrate the merits of CE-based enzymatic assays. Advantages and limitations of the CE-based enzymatic assays will be highlighted and briefly compared to LC-based ones of the same caliber. Furthermore, recently developed binding assays of lipases and kinases will be briefly discussed.

2. CE-based lipase assays

In this section, applications of CE utilizing lipases as model enzymes in drug screening, chiral resolution, organic synthesis and enzyme characterization will be reviewed. A brief comparison with LC-based approaches will be established when necessary in order to highlight on the advantages and limitations of the analytical techniques. Furthermore, binding assays of lipases will be briefly introduced.

2.1 General information about lipases

Lipases (EC 3.1.1.3) belong to the hydrolases class of enzymes that catalyze the hydrolysis of ester bonds such as those of triglycerides (TG) resulting in the release of free fatty acids (FFA) and monoglyceride (MG), facilitating the absorption of fats into the body (Figure 1) [39]. Several interesting applications have been described for lipases in different industrial fields such as in the baking, dairy and pharmaceutical industry, production of cosmetics and detergents, synthesis of bio-diesel or bioremediation processes [40–44]. Lipases-catalyzed reactions are rather straightforward but operate with a unique mechanism of activation at the aqueous-fat/organic interface (interfacial activation) [45,46]. Thanks to its versatility in operation modes and hyphenation tactics, CE is a suitable technique for monitoring reactions catalyzed by lipases where different types of products can be obtained.

2.2 Lipases activity and modulation

Assessment of enzymatic activity can be helpful in identifying the presence or prove the absence of an enzyme in a sample. Additionally, quantitative analyses of enzymatic reactions are crucial

for the understanding of the underlying mechanisms governing lipase reaction as well as the subsequent biological and chemical consequences [47]. Enzymatic assays and the screening for lipase inhibitors have been largely explored by CE [27,36,37,48–50] and HPLC [51–54].

The implication of CE in lipase-related studies was as early as the 1990s where it was used to determine the purity of lipases from crude specimen [55,56]. In 1998, B. Vallejo-Cordoba *et al.* introduced a CE assay to measure free fatty acids (FFA) in cream subjected to hydrolysis by lipases [57]. FA with chain lengths of 4 – 12 carbons (C₄-C₁₂) were detected by adding p-anisate to the 20 mM tris BGE as a chromophore using indirect UV detection at $\lambda = 270$ nm. Methylated beta-cyclodextrin (β -CD) was added to the BGE in order to enhance the solubility of FFA in the aqueous solution through the formation of inclusion complexes, as previously described by L. Szente *et al.* [58]. Conditions of the enzymatic reaction and CE separation are summarized in Table 1. The kinetics of cream fat hydrolysis into FFA, catalyzed by a commercial lipase isolated from *Rhizomucor miehei*, were followed by analyzing sample aliquots at different time periods for 60 min (Figure 2a).

The released FFA were analyzed using the CE method where a good separation of the individual FFA species was obtained which allowed their quantification using pre-constructed calibration curves. Figure 2b represents the electropherogram of resolved FFA species separated in only 10 min as anions of decreasing order of carbon chain length. Furthermore, it was revealed that short chain FFA (C₄, C₆ and C₈) were the most abundant compared to larger ones at different reaction times. The adopted CE method also permitted the detection and quantification of FFA in fresh cream subjected to a MeOH extraction protocol. Compared to the FFA-extracted cream, higher quantities of all FFA, especially those with short carbon chains, were detected in the lipolyzed one. These short chain FFA play an important role in determining the flavor of dairy products [59,60].

The developed CE method overcame the requirements of FFA derivatization or extraction, associated with chromatographic techniques such as gas chromatography (GC) and liquid chromatography (LC). The study demonstrated the possibility of customizing dairy flavors by blocking the lipase catalyzed hydrolysis of milk fat at specific times giving emphasis to short-chains FFA production and providing an index for assessing milk quality.

Gang Hao *et al.* described an LC-quadruple time-of-flight (Q-TOF) MS method for assaying microbial lipase activity [61]. The reaction mixture composed of lipase, triolein TG, 20% Triton-X and incubation buffer (IB) was incubated at 37°C before injecting aliquots of 2 μ L collected at

different time points into LC-MS and measuring the amount of liberated oleic FA by using an isotopically labeled [^{13}C]-oleic acid as an internal standard. LC was coupled to the Q-TOF MS by an electrospray ionization (ESI) source. Mass spectra of oleic acid ($m/z = 281.25$) and the internal standard ($m/z = 299.25$) were collected in the negative ionization mode at a capillary voltage of 2500 V. The method overcame the laborious radioactive or fluorescent labelling of the substrates and the high pH requirements associated with conventional assays. A limitation of the described assay compared to CE-based ones was the relatively high reagent concentrations which necessitated a 500-fold dilution of the aliquoted reaction samples prior to their analysis. Furthermore, the total injection volume of the samples collected sequentially over a period of 15 min ($5 \times 2 \mu\text{L}$) was one hundred-folds lower than the total volume of the reaction mixture (1 mL), which meant that most of the sample was wasted especially since triolein hydrolyzed spontaneously and had to be freshly prepared from stocks stored at freezing temperatures.

T. Koseki *et al.* [62] assayed the lipolytic activity of a recombinant lipase from filamentous fungi *Aspergillus oryzae* (rLipAO), purified from an expression vector. Hydrolysis of tributyrin, a natural TG found in butter, into butyrate was monitored using LC hyphenated to Q-TOF-MS and CE hyphenated to TOF-MS. The lipolytic activity of rLipAO was compared to that of tannase, an enzyme catalyzing the hydrolysis of ester and depside bonds, from the same fungal species. The hydrolysis reaction was measured through the detection of lingering tributyrin after the reaction by RP-LC-MS after injecting $1 \mu\text{L}$ of reaction mixture. CE-MS was used in the negative ionization mode to monitor the release of butyric acid at m/z 87.045. Reaction and CE separation conditions are summarized in Table 1. Figure 3 demonstrates the tributyrin hydrolysis reaction catalyzed by rLipAO. The electropherogram represents the detection of butyrate peak at a migration time of approximately 15 min in the presence of rLipAO. No butyrate peak was in the absence of rLipAO. The isolated protein rLipAO demonstrated lipolytic activity toward the tributyrin substrate after 5 hr incubation at 37°C whilst *A. oryzae* tannase showed no activity.

This study demonstrated the practicality of CE-MS and its complementarity to LC-MS for the characterization of the enzymatic activities of newly discovered proteins and protein fractions. Moreover, enzyme immobilization offers them a higher tolerance to variations in temperatures and pH and provides them with better storage stability [63,64]. It is argued that this increased tolerance compared to in-solution enzymes is brought about by the lower flexibility of the amino acid

conformation of the immobilized enzymes, protecting them from thermal and pH-mediated denaturation [63,65].

An online immobilized enzyme microreactor (IMER) was introduced by Y. Tang *et al.* in 2019 [66] to screen for lipase inhibitors. Pancreatic lipase (PL) was immobilized onto (3-aminopropyl)triethoxysilane (APTES)-treated silica of the inner capillary walls *via* cross-linking to a glutaraldehyde (GA) linker in three steps as illustrated in Figure 4a. The online enzymatic hydrolysis of 4-nitrophenyl acetate (4-NPA) was then followed by measuring the peak area of the 4-NP product spectrophotometrically at $\lambda = 400$ nm. Following the optimization of acetonitrile content in the enzymatic media, reaction pH and incubation time, the repeatabilities of the 4-NP product peak area and migration time were evaluated. Using the same capillary provided good peak areas and migration time repeatabilities (relative standard deviation or RSD < 5%) while the RSD obtained using different capillaries were slightly higher but were still within the acceptable range (< 15%) defined by international guidelines for validating analytical methodologies [67]. Immobilized lipase preserved 80% of its catalytic activity after 20 consecutive tests reflecting great stability of the immobilized enzyme (Figure 4b, left). The affinity of immobilized PL towards 4-NPA ($K_m = 2.7 \pm 0.29$ mM) was evaluated against a range of 4-NPA concentrations (0.6 - 7 mM) (Figure 4b, right) and was almost two-folds greater compared to that of PL in solution ($K_m = 4.65 \pm 1.23$ mM). This was attributed to a reduced steric hindrance between the immobilized PL molecules and thus an increased contact between PL and the 4-NPA substrate. The IMER was used to assay PL inhibition by orlistat, a reference PL inhibitor, as well as ten traditional Chinese medicine extracts at 10 mg mL⁻¹ by observing the decrease in 4-NP peak areas (Figure 4c). Conditions of the enzymatic reaction and CE separation are summarized in Table 1. IC₅₀ of orlistat was evaluated as 0.0097 μ M, which was globally in good agreement with the literature. Six out of the ten samples were demonstrated to possess mild to potent PL inhibition activity ranging from 21 to 70%. The developed method demonstrates the merits of enzyme immobilization, enhancing both the affinity and activity of immobilized PL towards the 4-NPA substrate compared to in-solution PL. Furthermore, the application of the method allowed rapid, automated and economic analysis of PL inhibitors in complex plant extracts. The co-migration of some plant components with the 4-NP product peak can be overcome by increasing the migratory distance to the detector. Another lipase immobilization approach was introduced shortly after by Jai Liu *et al.* [68]. Using the offline CE mode was used to search for inhibitors of immobilized *Candida rugose* lipase (CRL)

in traditional Tibetan medicines. CRL was attached onto titanium dioxide magnetic nanoparticles ($\text{Fe}_3\text{O}_4@\text{TiO}_2$) which provides an efficient mean of low-cost enzyme immobilization as well as the ability to separate the immobilized enzyme from the reaction medium due to the magnetic nature of such NP. The group demonstrated several optimizations performed to enhance CRL immobilization such as the pH, time and enzyme concentration. Furthermore, the activity of the immobilized enzyme towards 4-nitrophenyl palmitate (4-NPP) was compared to that of in-solution CRL. The release of 4-NP as a result of CRL-catalyzed hydrolysis of 4-NPP was monitored spectrophotometrically at $\lambda = 400$ nm. Reaction and CE separation conditions are summarized in Table 1. Compared to in-solution CRL, the immobilized enzyme was more active at high temperatures (40 - 50°C) and preserved most of its 4-NPP hydrolyzing activity after storage at 4°C for 30 days whereas in-solution CRL lost around 65% of its activity. Furthermore, immobilized CRL demonstrated higher affinity towards 4-NPP (2.51 mM) compared to CRL in solution (9.96 mM). The inhibition kinetics of immobilized CRL were investigated against a range of orlistat concentrations. A K_i value of 13.41 μM and an IC_{50} value of 4.37 mM was obtained for orlistat. Moreover, amongst 6 methanolic extracts of traditional Chinese medicines, *Oxytropis falcate* Bunge demonstrated considerable inhibition of immobilized CRL with 54 and 69% inhibition at 50 and 100 mg mL^{-1} , respectively. Eleven compounds were identified and isolated from *Oxytropis falcate* Bunge. They were screened individually for immobilized CRL inhibition and compared to that of orlistat at 50 and 100 μM . Six out of the eleven compounds had promising CRL inhibitory potentials similar to that of orlistat, which inhibited CRL by 64 and 82% at 50 and 100 μM , respectively. Kaempferol demonstrated superior inhibition to that of orlistat (92% at 50 and 100 μM). Kaempferol has been previously demonstrated as a CRL inhibitor and its inhibition has been attributed to the high number of hydroxyl group in addition to their location on the molecule [69]. In this study, lipase immobilization onto NP have shown to improve the enzyme's durability, stability, reusability and, its affinity and activity towards the 4-NPP substrate compared to in-solution lipases.

Y.-T. Zhu *et al.* introduced an HPLC-UV approach in 2014 to screen inhibition of porcine PL immobilized covalently onto magnetic nanoparticles (NP) [70]. Several techniques such as atomic force microscopy (AFM) and Fourier-transform infrared spectrometry (FT-IR) were used to characterize the NP and the covalent binding of PL onto them. Briefly, the amount of 4-NP liberated from the immobilized PL-catalyzed hydrolysis of 4-NPP,

was monitored at $\lambda = 317$ nm in the presence of reference PL inhibitors orlistat, (–)-epigallocatechin 3-O-gallate (EGCG) and (–)-epigallocatechin (EGC) and compared to that in their absence. The incubation of immobilized PL with the inhibitors was carried out offline prior to injection. IC₅₀ values of 0.64 ± 0.02 μ M and 55 ± 0.5 μ M were calculated for orlistat and EGCG, respectively, whereas no inhibitory effect was observed by EGC. As was the case in the previous examples containing immobilized lipases, NP-PL demonstrated superior endurance to pH and temperature changes as well as higher activity and affinity towards the 4-NPP substrate, compared to in-solution lipases as suggested by higher V_{\max} (6.40 vs 3.16 U mg⁻¹ enzyme) and lower K_m (0.02 vs 0.29 mM) values, respectively. The total volume of the reaction mixture (4 mL) used in this study by HPLC-UV were quite elevated and the retention time of the 4-NP product was relatively long (≈ 19 min) whereas only 5 min were needed using CE-based assays of immobilized lipases in the previous example.

Our group has recently developed and optimized the first homogeneous CE-based lipase assay utilizing simultaneous double detection in the offline and online modes [71]. No immobilization of PL or modifications of the capillary wall was needed. The reaction was monitored through the detection of both products of the hydrolysis of 4-nitrophenyl butyrate (4-NPB) substrate, namely 4-NP by spectrophotometry ($\lambda = 400$ nm) and butyrate by capacitively coupled contactless conductivity detector (C⁴D) (Figure 5a & b).

The capillary cartridge was supported by a home-made 3D-printed scaffold used to fasten both UV and C⁴D detectors and ensure the circulation of the capillary cartridge coolant (Figure 5c). Conditions of the online and offline CE-based assays are summarized in (Table 1). The Michaelis–Menten constant (K_m) was evaluated as 0.57 ± 0.03 and 0.59 ± 0.12 mM ($n = 3$) using 4-NP and butyrate, respectively. The maximum velocity (V_{\max}) was evaluated as 1.20 ± 0.13 and 0.71 ± 0.07 μ M s⁻¹ ($n = 3$) using 4-NP and butyrate, respectively. Using the offline assay, extracts from three plants, obtained *via* infusion in water, as well as a series of molecules isolated from oakwood and wine extracts were all screened for PL modulation activities at 1 mg mL⁻¹ ($n = 3$). Amongst the plant extracts, those from fresh leaves of *Crataegus oxyacantha* (hawthorn) demonstrated the strongest PL inhibition ($37 \pm 3\%$) whilst those from dry leaves of *Ribes nigrum* (black currant) demonstrated the highest activation ($37 \pm 1.5\%$). Amongst the compounds isolated from oakwood and wine extracts, two original triterpenoids were presented for the first time as potent PL inhibitors, $51 \pm 1\%$ by bartogenic acid and $57 \pm 4\%$ by 3-O-galloylbarrinic acid. This inhibitory

effect was attributed to the presence of galloyl moieties or absence of glucosyl ones at specific positions of the compounds. As far as we know, this is the only study that implicates CE-based PL assays in a homogeneous phase with the other reactants.

2.3 Enantioselective synthesis catalyzed by lipases

CE has been established as a successful technique for chiral separations through the use of a chiral selector in the BGE [72]. Lipases are known as chiral enzymes with stereo- and regioselective properties favoring the formation of either enantiomers [73].

K. Pomeisl *et al.* [74] described an offline CE-based heterogeneous lipase assay using immobilized lipase B from *Candida antarctica* (CALB) for the enantioselective resolution of *gem*-difluorinated alcohols. These alcohols serve as intermediates in the synthesis of bioactive molecules with potential anti-viral activities. The synthesis pathway of these fluorinated molecules is often complicated. Additionally, the bioactivities of these molecules strongly depend on their configuration. Lipase catalyzed enantioselective synthesis is thus an interesting approach for the production of difluorinated bioactive molecules from alcohol derivatives. The group monitored the progression of the transesterification reaction with time using CE/UV at $\lambda = 206$ nm. The racemic (R and S) 3-(benzyloxy)-1-difluoropropanol alcohol substrates and subsequent racemic ester products were detected and separated using sulfobutyl ether as a chiral selector in the phosphoric acid (pH 2.5) BGE. The CE method allowed monitoring of enantiomeric substrate and products in 14 min. The injection volume was very small (1-2 nL) making the method interesting in analyzing reactions with low yields. The group identified a change of enantioselectivity when changing the enzyme-to-substrate ratio from 1:1 to 5:1. They related these findings to the presence of three reaction steps: acetylation, hydrolysis and isomerization.

A. Schuchert-Shi and P. C. Hauser [75] demonstrated the enantioselective hydrolysis of serine and threonine amino acid esters by porcine PL using CE- C^4D . The use of conductimetry was essential due to the inability to detect non-aromatic amino by UV spectrophotometry. The enantioselectivity of the hydrolysis reaction was performed by temporal monitoring of the progression of the reaction through the formation of the D- and L- amino acid, products. An acidic BGE, 2 M acetic acid, containing 5 mM of the chiral selector (+)-(18-crown-6)-2,3,11,12-tetracarboxylic was used for the chiral analyses. The separation of the DL-serine methyl esters (SME) substrate from the DL-serine products and the enantiomeric resolution of D- and L- stereoisomers is demonstrated in

Figure 6.

The reaction was conducted by mixing PL with DL-SME or DL-threonine methyl esters (TME). The group demonstrated the increased selectivity of PL towards the L-isoforms of both amino acid methyl esters when assayed individually. Similarly, the enantioselectivity of PL was compared to that of wheat germ lipase (WGL) using DL-SME hydrolysis. A consensus was established for the favored production of L-serine by both PL and WGL with PL being more selective and having a higher reaction rate. Between TME and SME, PL activity was higher towards the L-isoforms of TME. This selectivity was related to a single structural difference manifested by a methyl group unique to threonine and not to serine. Indeed, separation of molecules that differ only in their three-dimensional configuration (stereoisomers) was possible with CE [76]. This was also demonstrated in the studies utilizing lipases to catalyze enantioselective hydrolysis of chiral substrates.

Recently, Y. Choi *et al.* described an HPLC-based analytical method to determine the integral stereoselectivity of lipases towards TG and DG [77]. This stereoselectivity considers the preference of lipase hydrolysis towards all three ester bonds on the acylglycerol (TG and DG) species. The detection required derivatization of the hydrolysis products with 4-nitrophenyl isocyanate (4-NPI). In order to determine the integral stereoselectivity of porcine PL, *Chromobacterium viscosum* lipase (CVL) and, *Pseudomonas fluorescens* lipase (PFL), the enantiomeric excess of 1,2-DG over 1,3-DG was measured at different stages of the hydrolysis reaction. Figure 7a represents the HPLC coupling to UV and evaporative light scattering detector (ELSD). The 1,2- and 2,3-DG enantiomers were quantified using HPLC-UV at $\lambda = 285$ nm after their derivatization. Using this method, it was shown that PL demonstrated no preference towards ester bonds at positions (pos) 1 or 3 of the TG substrate, hydrolyzing them equally. Pos 2 ester bonds were not hydrolyzed by PL. Moreover, a similar trend was observed for the hydrolysis of DG into MG. For CVL, a contrast between the stereoselectivity towards ester bonds of TG and DG was observed where the enzyme preferred pos 3 ester bonds over pos 1 in TG and the inverse in DG. As was the case for PL, CVL did not hydrolyze ester bonds at pos 2. Finally, PFL demonstrated hydrolysis of pos 2 ester bonds of TG. The stereoselectivity was thus in the order of ester bonds at pos 1, 2 and 3 of TG. The method did not permit the determination of the exact stereopreference of PFL towards DG isomers due to the presence of two possible hydrolysis sites on each isomer. These results are represented in Figure 7b. The HPLC-based methods demonstrated the ability to separate the different DG and MG isomers with good resolution and

separation factor (> 1). The isomers were then quantified using either HPLC-UV or HPLC-ELSD which permitted the assessment of integral stereoselectivity of lipases from three biological sources.

A drawback of the method was the need for isomer derivatization. Furthermore, although all three DG isomers derivatives were detected in 13 min, the detection of MG isomers required the analyses time to be extended to over 20 min. The reaction volume for HPLC-UV analyses (300 μ L) was elevated compared to CE-based assays. A powerful green chromatographic technique to be used for enantioresolution is supercritical fluid chromatography (SFC) where supercritical carbon dioxide, possessing properties of both liquid and gas, is used as the mobile phase [78].

The previous examples demonstrate the efficiency of using CE for enantiomeric separation of molecules, simply by adding a chiral selector in the BGE, and its power to separate products obtained after enzymatic reaction in a relatively short time with minimal volume requirement.

2.4 Organic synthesis

The use of CE to monitor synthesis reactions is a promising prospect given the flexibility and the low sample consumption of the technique. Furthermore, lipases have been used in biocatalyzed organic synthesis reactions given their high catalytic activity, wide range of substrate specificity and most importantly, their tolerance to high organic media [79].

W. Liu *et al.* [80] compared the activities of porcine PL immobilized onto different forms of porous materials (metal-organic framework or MOF and SBA-15) by CE-UV through monitoring the formation of anticoagulant-molecule, warfarin. The PL catalyzed synthesis reaction was carried out by incubating PL with 4-hydroxycoumarin and benzylideneacetone, in methanol for 1 day at 50°C (Figure 8a). Reaction and CE conditions are summarized in Table 1. At the end of the reaction, the solution was centrifuged for 5 min to separate the produced warfarin and residual substrates into the supernatant and the carrier-PL complex into the residue.

This allowed the reusability of the immobilized PL. The supernatant was injected into the capillary (0.5 psi x 3 sec; 3 nL) and a separation voltage of 28 kV was applied to separate the warfarin product from the substrates using a borax buffer containing sodium dodecyl sulfate (SDS) as BGE (pH 8.5). An example of the obtained electropherograms with PL immobilized onto MOF is presented in Figure 8b. The warfarin yields by each of the PL immobilized onto 4 different MOFs and SBA-15 in addition to in-solution PL were compared to assess catalytic activity and storage

of the immobilized enzyme. Compared to in-solution, all immobilized PL had higher activities reflected by higher warfarin yields that did not change dramatically upon reusing after 5 cycles. PL-MOFs had higher warfarin synthesizing activities compared to PL-SBA-15. The majority of warfarin yield (65%) were maintained by PL-MOFs after storage for 35 days at 4°C. Additionally, the RSD of warfarin yields using three batches of each PL-MOFs and their use across five cycles was inferior to 3 % reflecting high catalytic stability. With 104 μ L total reaction volume, 3 μ L injection volume and the ability to reuse the immobilized enzyme, the CE method for monitoring warfarin synthesis was highly economic providing rapid separation of warfarin from the other reactants in under 8 min.

The miniaturization of such organic reactions onto microchip systems with continuous flow conjugated to appropriate detection techniques should be considered due to the advantages provided at such scales especially the shorter reaction times [81].

2.5 Binding assays of lipases

In 2019, I. Hamdan *et al.* applied affinity CE to monitor changes in the migration times and peak shapes of PL upon binding to certain drugs, orlistat or a combination of both [82]. CE was used to confirm findings obtained using conventional spectrophotometric PL inhibition assays and docking studies. Some of the tested drugs demonstrated synergism in inhibitory activity where the addition of orlistat enhanced the overall inhibition. This was attributed to the binding mode of these drugs to PL where the active site, *i.e.* orlistat binding site, remained exposed. Other drugs demonstrated antagonism when combined with orlistat where the overall inhibition diminished due to interferences with orlistat binding to the active site of PL. Orlistat, the tested drugs or both were added to the 50 mM phosphate buffer (pH 6.8) containing 15% (v/v) ACN and 16.7% (v/v) MeOH as BGE which was then used to fill the capillary. PL was then injected into the capillary. As shown in Figure 9, PL (0.1 g L⁻¹) injected electrokinetically (18 kV \times 15 s) into a capillary filled with blank BGE (no ligands) was detected at 5.6 min by UV at λ = 205 nm. Once orlistat alone was added to the BGE, a shift of PL migration time from 5.6 to 6.5 min was observed. This was attributed to the binding of orlistat to PL favoring the migration of the complex towards the anode, opposite to the direction of the EOF, and thus slowing down its migration in the capillary by almost 1 min. Similarly, the presence of the tested drugs in the BGE resulted in a similar change to PL in the capillary. When orlistat was present in combination with the drugs in the BGE, the

migration times shifts and peak shape changes were more drastic compared to the drugs or orlistat alone (Figure 9a). One sole drug, dinitrosalicylic acid (DnS), did not demonstrate any significant changes to the electropherograms upon addition of orlistat. This observation agreed with the results obtained using PL inhibition assays and molecular docking studies (Figure 9b). DnS was shown to bind strongly to Ser-152 of PL's active site which happens to be orlistat's binding site. Thus, the overall inhibitory potential was reduced.

An interesting biophysical technique on the rise and used to evaluate biomolecular binding affinities is microscale thermophoresis (MST) [83]. MST is based on the differential thermodiffusion of bound and unbound species which is governed by the size, charge and solvation of the analytes [83–85]. The technique is non-separative allowing the determination of K_d with high sensitivity (in pM) in under 30 min and consuming miniscule amounts of samples ($\approx 4 \mu\text{L}$ for each ligand concentration tested). Furthermore, using MST provides the analyst with the freedom of choice of the buffer where practically any convenient solution or complex biological fluids can be used. It has been previously applied for the evaluation of interactions between *E. Coli* AK and ligands [86] as well as nucleoside diphosphate kinase (NDPK) and nucleoside analogs [87]. Additionally, our group used MST to evaluate the binding affinity between human neutrophil elastase (HNE) and ursolic acid, a reference inhibitor of HNE ($K_d = 2.72 \pm 0.66 \mu\text{M}$) [88].

Recently, our group developed for the first time an MST-based binding assay to evaluate the binding affinities of small ligands towards lipases from crude pancreatic extracts [89]. The investigated ligands were purified from oakwood extracts and have been previously shown to affect the activity of lipases either activating or inhibiting it using a CE-based assay [71]. The MST protocol was optimized at different levels including the labeling protocol, storage and analysis temperature and target concentrations. Once optimized, the MST method was used to titrate a fixed concentration of the labeled lipases against a range of ligand concentrations. The K_d values were evaluated for bartogenic acid (BA; $K_d = 1327 \pm 700 \text{ nM}$), 3-O-galloylbarrinic acid (3-GBA; $K_d = 500 \pm 300 \text{ nM}$) and Quercotriterpenoside-I (QTT-1; $K_d = 31 \pm 21 \text{ nM}$). The augmented standard errors reflect poor repeatabilities of K_d evaluation possibly resulting from the fact that several types of lipases are present simultaneously in the crude extracts. Enhancing the purity of the 50 kDa PL, present in the extracts, by ammonium sulfate precipitation was successful although not compatible with the MST labeling protocol. The obtained information is strictly restricted to the binding and do not reflect the type of modulation this binding introduces to the lipase's activity. This became

problematic when the standard lipase inhibitor, orlistat, was considered. Due to the fact that orlistat induces inhibition through covalent binding to the lipases active site and that MST are not suitable to evaluate such type of irreversible binding interaction, using results from MST alone would give the impression that orlistat and lipases do not interact.

The complementary use of activity-based assays by CE and binding affinity-based assays by MST thus provides a better understanding of the molecular mechanism and paints a clearer image of the modulation of catalytic activity resulting from ligand bindings.

The developed assay was successful in indicating a binding interaction between lipases and small oakwood ligands despite using lipases from crude extracts which is a complex source of these enzymes.

3. CE-based nucleoside kinase assays

This section will review some of the CE-based assays of nucleoside kinases. Unlike lipases, applications of nucleoside kinases are mainly exclusive to scientific and pharmaceutical research. Similar to the previous section, a brief comparison with LC-based approaches will be established and nucleoside kinase binding assays will be briefly introduced.

3.1 General information about nucleoside kinases

Kinases (EC 2.7.x.x) belong to the family of phosphotransferases catalyzing the transfer of an energetic phosphate group from a donor such as nucleotide triphosphates (NTP) toward an acceptor. Kinases are divided into classes based on the type of phosphate group acceptors (*e.g.*: proteins or nucleosides). Nucleoside kinases (EC 2.7.4.x) are essential for the phosphorylation of nucleosides and nucleoside phosphates (nucleotides) playing major roles in processes such as the nucleoside salvage pathways and DNA replication [90]. Figure 10 depicts the phosphorylation of a nucleoside, thymidine, by thymidine kinase (TK), producing thymidine monophosphate (TMP) and ADP. The phosphorylation of TMP to thymidine triphosphate (TTP) is then catalyzed by other types of cellular nucleoside kinases. As is the case with other types of kinases, this reaction requires the presence of a divalent metal cation to neutralize the negative charges of the phosphate groups [90]. In this section, applications of CE for studies involving nucleoside kinases as models of more complex enzymatic reactions with applications in scientific and pharmaceutical research will be presented. Furthermore, kinases in general are often expensive to purchase and their production

require tedious work and may be time consuming. Therefore, it of interest to the manipulator to use a technique such as CE that requires lower volumes of the enzymes in order to economize their consumption.

3.2 Nucleoside kinases activity and modulation

In 1996, S. Banditelli *et al.* described a CE-based assay to monitor the activity of cytosolic 5'-nucleotidase. Although not a kinase, cytosolic 5'-nucleotidase is a bifunctional enzyme demonstrating phosphotransferase in addition to hydrolase activities [91]. Through the use of a single CE-UV assay, both activities of 5'-nucleosidases were simultaneously monitored. The method, summarized in Table 2, demonstrated an efficient separation of a mixture consisting of several bases, nucleosides and nucleoside mono, di and triphosphates. The overall activity (phosphatase + kinase) of the enzyme increased in the presence of a nucleoside phosphate acceptor as demonstrated by the higher conversion of dGMP to dG in the presence of a nucleoside acceptor such as inosine. Moreover, phosphorylation of deoxycytosine, an analog of adenosine used as a chemotherapeutic drug, by the 5'-nucleotidase was demonstrated for the first time. This CE-UV method was simple, rapid and required no labeling or modification of the substrates. Additionally, the detection and efficient separation of the substrates and the products of both reactions catalyzed by 5'-nucleotidase allowed the determination of the reaction rates corresponding to each activity in a relatively short time (12 min) without the need of large sample quantities (10 nL).

H.-F. Tzeng *et al.* developed a CE-UV assay for measuring the activities of thymidine kinase (TK) and thymidine monophosphate kinase (TMPK), simultaneously [92]. The method was optimized for the detection of TMP and thymidine diphosphate (TDP), the products of thymidine phosphorylation by TK and TMP phosphorylation by TMPK, respectively. A fused-silica bubble cell capillary with an extended light path length of 150 μm to improve detection sensitivity [93]. Ethylenediaminetetraacetic acid (EDTA) was added in order to chelate Mg^{2+} co-factor ions which were censured for the considerable ATP peak fronting due to the formation of ATP-Mg^{2+} complexes. This resolved the ATP and TDP peaks which migrated close to one another. Mixing the analyzed sample with NaCl and 66.7% ACN (v/v) prior to CE injection brought about several improvements to the CE separation efficiency, peak shapes and mediated a sample stacking effect. Indeed, slightly lower currents were achieved with ACN in addition to a 73% increase in the apparent mobility difference between TDP and ATP species, enhancing the resolution of their

peaks by more than 100%. A 3-fold increase in the theoretical plate counts was achieved upon addition of 20 mM NaCl to the sample treated with ACN. The optimized method was applied to simultaneously detect TK and TMPK activities of the white spot syndrome virus (WSSV)-infected insect cell line. Conditions of the enzymatic reaction as well as CE separation are summarized in Table 2. After 10 min incubation of the cell protein extract with the reaction buffer at 37°C, TMP and, to a lesser extent, TDP were detected confirming the presence of both TK and TMPK activities (Figure 11). An additional 10 min incubation period at 37°C was sufficient to obtain a 170% increase of TDP production, verifying the presence of TMPK activity in WSSV-infected cells. The CE method provided a highly repeatable, rapid (6 min) and efficient separation of different nucleosides in lysated cells. C. C. Liu *et al.*[94] described a CE-ESI-MS assay to monitor the phosphorylation of lamivudine, an anti-retroviral drug, in human cell lines. Here, the negative ionization mode was used as it provided similar detection sensitivities of both unphosphorylated and phosphorylated nucleosides. The CE-MS method involved the use of a volatile ammonium acetate solution as BGE. This allowed the separation of GMP from dGMP standards, differing only by the presence of a hydroxyl group in GMP (Figure 12a). The developed method was then applied to monitor the production of phosphorylated lamivudine metabolites in human cell line extracts. Lamivudine is a cytosine analogue that is phosphorylated sequentially by cellular kinases into active lamivudine triphosphate. The latter competes for incorporation into the RNA by reverse transcriptases of viruses such as the human immunodeficiency virus (HIV) or hepatitis B virus (HBV), blocking their replication. Conditions of the enzymatic reaction and CE-MS analysis are summarized in Table 2. All three phosphorylated metabolites of lamivudine as well as lamivudine itself were detected and separated in under 15 min verifying its activation in the human cell lines (Figure 12b). In both previous examples, the developed CE-based nucleoside kinase assays were validated through their application to living cells. The higher degree of complexity that cells provide relative to *in-vitro* enzymatic assays attests to the credibility of the developed assays and the interest of using CE for such analyses.

In 2006, J. Iqbal *et al.* described the development of three CE-based methods (Table 2) to assay the activity and inhibition of adenosine kinase (AK) [95]. In the first method (Method A), the micellar electrokinetic chromatography (MEKC) mode of CE-UV analysis was implemented through the use of a BGE containing SDS. The MEKC-based method was used to test seven adenosine nucleoside analogs, differing in the nature of substitution at position 2, as alternative

substrates of adenosine (Figure 13a). Only pyrrolidinyl- and isopropylamino-substituted analogues showed relevant phosphorylation by AK, 53 and 81% respectively, compared to that of natural AK substrate, adenosine. The combination of alkaline pH and high SDS content of the BGE (Table 2) ensured the separation of the analogue substrates of AK-catalyzed phosphorylation reactions and their phosphorylated products. The second method (Method B) was quite similar to the first one except for the BGE and the internal standard used (Table 2). It was applied to assess the inhibition of AK by three standard AK inhibitors. A-134974, an analog of adenosine, was identified as the most potent inhibitor according to the K_i values obtained using the developed CE-based bovine AK assay as well as radioactive assays for bovine and human AK (Figure 13b). The inhibition was assessed by measuring the extent of diminishing of the AMP product peak, detected at 7 min, relative to a control AK-catalyzed reaction without inhibitors. The migration time of the AMP peak was reduced by 2 min by increasing the pH of the BGE from 7.5 to 8.5. This is mainly due to the increase in the magnitude of EOF sweeping all analytes towards the detector. The second method thus permitted, in only 5 min, the calculation of kinetic inhibition parameters used to rank AK inhibitors for their effectiveness.

Both of the methods described so far (A and B) involved carrying out AK-catalyzed reactions offline. In the third method (Method C), the AK assay was carried out using the online CE-mode. The capillary was coated with polyacrylamide to neutralize the silica charges on its walls and thus to limit the interaction between charged groups on proteins and the capillary wall, a phenomenon that often results in poor repeatabilities of migration times [96]. Furthermore, the use of a non-alkaline BGE was necessary, since at high pH values, the neutral coating is less stable. For on-line assay, a plug of the IB was first injected followed by sequentially injecting the enzymatic reactants. The injection sequence was terminated by the injection of an IB plug and finally BGE. The partial filling of the capillary with the IB plugs at the beginning and the end of the injection sequence aims to isolate the reaction components from the BGE which could interfere with the reaction due to its different pH. The reactants were mixed *via* EMMA after which the AMP product was allowed to accumulate. The K_i values of the inhibitors obtained by this online assay agreed with those obtained by the offline assay as well as by conventional radioactive assays where A-134974 was the most potent inhibitor (Figure 13b). The online AK inhibition assay (method C) allowed the adaptation of an automated, more economic form of the inhibition assays.

A similar example of this adaptability of CE was introduced a year later by the same group where they introduced an optimized CE-UV approach to assay TK activity of the herpes simplex virus (HSV) [97]. The phosphorylated product (dTMP) was detected in less than 7 min followed directly by the UMP standard. However, interactions between charged protein groups of TK and the silanol groups of the uncoated capillary led to variations in migration times and a decrease of the separation quality and efficiency (Figure 14a). Therefore, the authors adapted the method by masking the charged silanol groups by a polyacrylamide coating (Figure 14b). Indeed, a drastic reduction in the RSD of migration times of dTMP was observed with coated capillaries (16-fold lower, $n = 12$, Figure 14a). Furthermore, since the use of a neutral capillary required the reduction of the BGE's pH, the BGE's ionic strength was increased to achieve good peak resolution in short time. The use of electrokinetic injection allowed sample pre-concentration of anionic species and increased sensitivity by approximately 7-fold (Figure 14a). Concerning the inner diameter of the capillary, a higher diameter prompts higher detection sensitivities. However, the sensitivities of 75 μm capillaries were worse as more buffer ions are being introduced into the capillary by electrokinetic injection (Figure 14a). The final conditions of the enzymatic reaction and CE separation are summarized in Table 2. The optimized CE method was applied to assess 3 nucleoside analogues, acyclovir (ACV), (E)-5-(2-bromovinyl)-2'-deoxyuridine (BVDU) and ganciclovir (GCV), as substrates of HSV TK (Figure 14c). In this example, parameters enhancing the sensitivity of nucleotide detection as well as the repeatability of migration times by CE-UV were adapted through implementing different strategies. The CE-method was adequately applied in estimating kinetic parameters of each substrate which were in good agreement to previously published values. Additionally, it was possible to assay the nature of TK inhibition by ACV using the same method in around 6 min.

Similarly, our group applied a CE-UV method to determine the catalytic efficiency of human TMPK [98]. The catalytic efficiency is measured as the ratio of K_{cat} to K_{m} which reflects the effectiveness of the enzyme towards a particular substrate [99]. The catalytic efficiency of TMPK obtained *via* CE towards TMP was then compared to that obtained using either flow injection analysis coupled to high resolution mass spectrometry or spectrophotometric assays. The concentration of the BGE, ammonium acetate, was relatively high in order to limit interactions between the solutes and the capillary wall and enhances the repeatabilities of migration times [100]. The TMPK enzymatic reaction was carried out in the presence of low concentrations of

MgCl₂ and ATP (co-factors) similar to those of FIA-HRMS analyses, as a compromise between reduced ion suppression and adequate TMPK activity. The IB was a more diluted version of the BGE to mediate a stacking effect due to the differences in conductivities of the injected sample plug and the surrounding BGE [100,101]. This in turn enhances the shapes of the peaks and the sensitivity of detection. Reaction and CE separation conditions are summarized in Table 2. This method demonstrated the feasibility of carrying out kinetic evaluation of kinases using simply CE-UV. The catalytic efficiency of the TMPK determined by CE-UV was in the same order of magnitude compared to that determined by FIA-HRMS and conventional spectrophotometric assays as depicted in Figure 15.

Concerning LC-based nucleoside kinase assays, only few examples can be found. This may be due to the complex nature of the nucleoside kinase reaction and its media where analytes differing by a single phosphate group may be difficult to separate. Additionally, the fact that most LC-based analyses require the use of organic solvents is a hindering factor in the face of the development of an online LC-based enzymatic assay. N. Malartre *et al.* introduced an HPLC-UV assay for monitoring the phosphorylation activity of several different mutant variants of HSV-TK against endogenous deoxythymidine and ACV [102]. The detection of the phosphorylated products was possible in under 5 min, linear up to 0.22 mM with high sensitivity (LOD \approx 0.12 μ M). Based on the phosphorylation activity of the mutant TK towards both deoxythymidine and ACV relative to that of the wild-type TK, the proteins were classified into different classes providing means to better understand antiviral resistance developed by HSV towards ACV on a genotypic and phenotypic level.

Recently, C. Machon *et al.* introduced the first LC-HRMS assay to study 10 metabolites of 5-fluorouracil (5-FU), a chemotherapeutic drug used to treat several types of cancers [103]. The LC-MS method was first optimized for the detection of the different metabolites. The retention times of some of the 5-FU metabolites were either very close or similar. 5-FU sequential phosphorylation in HCT116 cells, human colon cancer cells, was confirmed by the indirect detection of 5-FUTP metabolites. The developed method was demonstrated to be highly sensitive (in pg), selective (discriminating 5-FU metabolites from endogenous ones) and linear (over a range of 0.5 - 3 million cells) for the detection of 5-FU metabolites. Although the method demonstrated a great selectivity towards 5-FU metabolites, due to the detection of specific fragmentation patterns of fluorine-containing metabolites, the separation efficiency was rather low. This is a common limitation of

porous graphitic carbon columns, used in this study, were upon usage, loss of resolution and retention capability is observed [104].

The abundance of CE-based nucleoside kinase assay relative to LC-based assays is a testimony of the better adequacy of the former. CE have better adaptability and flexibility to resolve possible issues. Furthermore, the low volume requirements and the little to no need for organic solvents promote CE as an excellent separative technique for enzymatic analysis.

3.3 Binding assays of nucleoside kinases

One of the few binding assays of nucleoside kinases was developed by J. V. Pagaduan *et al.* using a microchip electrophoresis to detect and quantify TK-1 in an immunocomplex using an anti-TK-1 antibody (Ab) [105]. The assay was coupled to laser-induced fluorescence for the detection of fluorescein isothiocyanate (FITC)-coupled Ab. The most suitable channel length was 5 mm as it was sufficient for the separation of the unbound Ab from the TK-1/Ab immunocomplex. The miniaturized assay was able to detect low concentrations (80 nM) of the immunocomplex in only 20 s. This assay however, was not applicable in its current form for the detection of TK-1 in serum samples since the physiological or pathological concentrations of the enzyme were far lower than the assay's detection limits (in the order of pM). Sample pre-concentration is one approach that would allow the application of the developed miniaturized ME assay for determination of TK-1 in biological samples.

4. Conclusion

In this review, the flexibility and reliability of CE for monitoring the catalytic activity reactions and screening for potential modulators were demonstrated through the use of lipases which produces a variety of products with different physical and chemical properties, and nucleoside kinases which are precious and scarce samples when available. In-solution as well as immobilized enzymes were successfully assayed using both offline and online CE modes coupled to different detection techniques such as UV spectrophotometry, LIF, C⁴D and MS. The highly efficient separation of the reaction components offered by CE comes in handy especially when the substrates and products of the reaction are indiscernible from each other by standard spectrophotometric approaches. The use of a wide array of synthetic and natural substrates was possible and the modulation assay involved the use of various samples that ranged in complexity

from crude plant extracts and cell lysates to isolated and purified molecules. A possible drawback encountered in some of the examples is associated with the use of complex samples which may lead to less reliable results especially when using online CE-based assays. Compared to chromatographic-based assays of lipases and nucleoside kinases, CE-based assays were faster, required lower reaction and injection volumes and needed no organic solvents. The use of affinity assays with the CE-based activity assays, complementarily, allows a better understanding of the molecular mechanism behind ligand binding to the enzyme and of the modulation of its activity. All these advantages conveyed by CE should expand its use in different application fields of pharmaceutical and scientific research.

5. Declaration

Authors' contribution

Both G. Al Hamoui Dit Banni and R. Nehmé contributed equally to this work.

Conflicts of interests

The authors declare that there is no conflict of interests.

Acknowledgements

The authors would like to thank the Région Centre Val de Loire (PhD fellowship of G. Al Hamoui Dit Banni) and the Labex SynOrg (ANR-11- LABX-0029) for financial support.

6. References

- [1] G. Kapoor, S. Saigal, A. Elongavan, Action and resistance mechanisms of antibiotics: A guide for clinicians, *J Anaesthesiol Clin Pharmacol.* 33 (2017) 300–305. https://doi.org/10.4103/joacp.JOACP_349_15.
- [2] Z. Lou, Y. Sun, Z. Rao, Current progress in antiviral strategies, *Trends Pharmacol. Sci.* 35 (2014) 86–102. <https://doi.org/10.1016/j.tips.2013.11.006>.
- [3] A. Sreedhar, Y. Zhao, Dysregulated metabolic enzymes and metabolic reprogramming in cancer cells (Review), *Biomed Rep.* 8 (2018) 3–10. <https://doi.org/10.3892/br.2017.1022>.
- [4] R. Nehmé, H. Nehmé, T. Saurat, M.-L. de Tauzia, F. Buron, P. Lafite, P. Verrelle, E. Chautard, P. Morin, S. Routier, H. Bénédicti, New in-capillary electrophoretic kinase assays to evaluate inhibitors of the PI3k/Akt/mTOR signaling pathway, *Anal. Bioanal. Chem.* 406 (2014) 3743–3754. <https://doi.org/10.1007/s00216-014-7790-z>.
- [5] B. Bonamichi, E.B. Parente, R.B. dos Santos, R. Beltzhoover, J. Lee, J.E.N. Salles, The challenge of obesity treatment: a review of approved drugs and new therapeutic targets, *J. Obes. Eat. Disord.* 4 (2018) 1–10. <https://doi.org/10.21767/2471-8203.100034>.
- [6] S. Fayad, P. Morin, R. Nehmé, Use of chromatographic and electrophoretic tools for assaying elastase, collagenase, hyaluronidase, and tyrosinase activity, *J. Chromatogr. A.* 1529 (2017) 1–28. <https://doi.org/10.1016/j.chroma.2017.11.003>.
- [7] J. Strelow, W. Dewe, P.W. Iversen, H.B. Brooks, J.A. Radding, J. McGee, J. Weidner, Mechanism of action assays for enzymes., in: S. Markossian, G.S. Sittampalam, A. Grossman, K. Brimacombe, M. Arkin, D. Auld, C.P. Austin, J. Baell, J.M.M. Caaveiro, T.D.Y. Chung, N.P. Coussens, J.L. Dahlin, V. Devanaryan, T.L. Foley, M. Glicksman, M.D. Hall, J. V Haas, S.R.J. Hoare, J. Inglese, P.W. Iversen, S.D. Kahl, S.C. Kales, S. Kirshner, M. Lal-Nag, Z. Li, J. McGee, O. McManus, T. Riss, P. Saradjian, O.J.J. Trask, J.R. Weidner, M.J. Wildey, M. Xia, X. Xu (Eds.), *Assay Guid. Man.*, Bethesda (MD), 2004.
- [8] M. Zeilinger, F. Pichler, L. Nics, W. Wadsak, H. Spreitzer, M. Hacker, M. Mitterhauser, New approaches for the reliable in vitro assessment of binding affinity based on high-resolution real-time data acquisition of radioligand-receptor binding kinetics, *EJNMMI Res.* 7 (2017) 13. <https://doi.org/10.1186/s13550-016-0249-9>.
- [9] P.J. Tonge, Quantifying the interactions between biomolecules: guidelines for assay design and data analysis, *Infect. Dis.* 5 (2019) 796–808. <https://doi.org/10.1021/acsinfecdis.9b00012>.
- [10] A. Cornish-Bowden, *Fundamentals of enzyme kinetics*, Elsevier Science, Amsterdam, ND, 2014. <https://books.google.fr/books?id=c4GQBQAAQBAJ>.

- [11] H. Bisswanger, 2: General aspects of enzyme analysis, in: *Pract. Enzymol.*, Wiley-Blackwell, 2012.
<https://doi.org/10.1002/9783527659227>.
- [12] G.A. Holdgate, T.D. Meek, R.L. Grimley, Mechanistic enzymology in drug discovery: a fresh perspective, *Nat. Rev. Drug Discov.* 17 (2018) 115–132.
<https://doi.org/10.1038/nrd.2017.219>.
- [13] G.W. Caldwell, Z. Yan, W. Lang, J.A. Masucci, The IC 50 concept revisited, *Curr. Top. Med. Chem.* 12 (2012) 1282–1290.
<https://doi.org/10.2174/156802612800672844>.
- [14] J. Chapman, A.E. Ismail, C.Z. Dinu, Industrial applications of enzymes : recent advances, techniques, and outlooks, *Catalysts.* 8 (2018) 1–26.
<https://doi.org/10.3390/catal8060238>.
- [15] P.J.T. Dekker, D. Koenders, M.J. Bruins, Lactose-free dairy products: market developments, production, nutrition and health benefits, *Nutrients.* 11 (2019) 1–14.
<https://doi.org/10.3390/nu11030551>.
- [16] F.N. Niyonzima, S. More, Preparative biochemistry and biotechnology detergent-compatible proteases : Microbial production , properties , and stain removal analysis, *Prep. Biochem. Biotechnol.* 45 (2014) 233–258. <https://doi.org/10.1080/10826068.2014.907183>.
- [17] R. Nehmé, P. Morin, Advances in capillary electrophoresis for miniaturizing assays on kinase enzymes for drug discovery, *Electrophoresis.* 36 (2015) 2768–2797.
<https://doi.org/10.1002/elps.201500239>.
- [18] N.S. El-Safory, A.E. Fazary, C.K. Lee, Hyaluronidases, a group of glycosidases: Current and future perspectives, *Carbohydr. Polym.* 81 (2010) 165–181.
<https://doi.org/10.1016/j.carbpol.2010.02.047>.
- [19] M. Stoytcheva, G. Montero, R. Zlatev, J.Á. León, V. Gochev, Analytical methods for lipases activity determination: A Review, *Curr. Anal. Chem.* 8 (2012) 400–407.
<https://doi.org/10.2174/157341112801264879>.
- [20] C.A. Espinosa-Leal, S. Garcia-Lara, Current methods for the discovery of new active ingredients from natural products for cosmeceutical applications, *Planta Med.* 85 (2019) 535–551.
<https://doi.org/10.1055/a-0857-6633>.
- [21] J.F. Glickman, 1. Assay development for protein kinase enzymes, in: S. Markossian, G. Sittampalam, A. Grossman, K. Brimacombe, M. Arkin, D. Auld, C. P. Austin, J. Baell, J.M.M. Caaveiro, T. D.Y. Chung, N. P. Coussens, J. L. Dahlin, V. Devanaryan, T. L. Foley, M. Glicksman, M. D. Hall, J. V. Haas, S. R.J. Hoare, J. Inglese, P. W. Iversen, S. D. Kahl, S.C. Kales, S. Kirshner, M. Lal-Nag, Z. Li, J. McGee, O. McManus, T. Riss, P. Saradjian, O.J.J. Trask, J. R. Weidner, M. Jo Wildey, M. Xia, X. Xu (Eds.), *Assay Guid. Man.*, Eli Lilly & Company and the National Center for Advancing Translational Sciences, Bethesda (MD), 2004: pp. 1–19. <http://www.ncbi.nlm.nih.gov/pubmed/22553863>.
- [22] Y. Wang, H. Ma, Protein kinase profiling assays: A technology review, *Drug Discov. Today*

Technol. 18 (2015) 1–8.
<https://doi.org/10.1016/j.ddtec.2015.10.007>.

[23] S. Lanka, A. Pradesh, J. Naveena, L. Latha, A short review on various screening methods to isolate potential lipase producers: Lipases-the present and future enzymes of biotechindustry, *Int. J. Biol. Chem.* 9 (2015) 207–219.
<https://doi.org/10.3923/ijbc.2015>.

[24] C. Peña-García, M. Martínez-Martínez, D. Reyes-Duarte, M. Ferrer, High throughput screening of esterases, lipases and phospholipases in mutant and metagenomic libraries: A Review, *Comb. Chem. High Through. Scr.* 19 (2016) 605–615.
<https://doi.org/10.2174/1386207319666151>.

[25] F. Hasan, A.A. Shah, A. Hameed, Methods for detection and characterization of lipases: A comprehensive review, *Biotechnol. Adv.* 27 (2009) 782–798.
<https://doi.org/10.1016/j.biotechadv.2009.06.001>.

[26] J.P. Hughes, S.S. Rees, S.B. Kalindjian, K.L. Philpott, Principles of early drug discovery, *Br. J. Pharmacol.* 162 (2011) 1239–1249.
<https://doi.org/10.1111/j.1476-5381.2010.01127.x>.

[27] M. Cheng, Z. Chen, Recent advances in screening of enzymes inhibitors based on capillary electrophoresis, (2018).
<https://doi.org/10.1016/j.jpha.2018.05.002>.

[28] N. Banke, K. Hansen, I. Diers, Detection of enzyme activity in fractions collected from free solution capillary electrophoresis of complex samples, *J. Chromatogr. A.* 559 (1991) 325–335.
[https://doi.org/10.1016/0021-9673\(91\)80082-R](https://doi.org/10.1016/0021-9673(91)80082-R).

[29] H. Nehmé, Etude des réactions enzymatiques par électrophorèse capillaire, Etude des réactions enzymatiques par électrophorèse capillaire, PhD Thesis, Université d'Orléans, 2013.

[30] J. Bao, F.E. Regnier, Ultramicro enzyme assays in a capillary electrophoretic system, *J. Chromatogr. A.* 608 (1992) 217–224 .
[https://doi.org/10.1016/0021-9673\(92\)87127-t](https://doi.org/10.1016/0021-9673(92)87127-t).

[31] B.J. Harmon, D.H. Patterson, F.E. Regnier, Mathematical treatment of electrophoretically mediated microanalysis, *Anal. Chem.* 65 (1993) 2655–2662.
<https://doi.org/10.1021/ac00067a018>.

[32] V. Okhonin, X. Liu, S.N. Krylov, Transverse diffusion of laminar flow profiles to produce capillary nanoreactors, *Anal. Chem.* 77 (2005) 5925–5929.
<https://doi.org/10.1021/ac0508806>.

[33] Y. Wang, D.I. Adeoye, E.O. Ogunkunle, I.A. Wei, R.T. Filla, M.G. Roper, Affinity capillary electrophoresis: A critical review of the literature from 2018 to 2020, *Anal. Chem.* 93 (2021) 295–310.
<https://doi.org/10.1021/acs.analchem.0c04526>.

[34] S. El Deeb, H. Wätzig, D.A. El-Hady, Capillary electrophoresis to investigate

biopharmaceuticals and pharmaceutically-relevant binding properties, *Trends Anal. Chem.* 48 (2013) 112–131.

<https://doi.org/10.1016/j.trac.2013.04.005>.

- [35] D.O. Lambeth, W.W. Muhonen, High-performance liquid chromatography-based assays of enzyme activities., *J. Chromatogr. B Biomed. Appl.* 656 (1994) 143–157. [https://doi.org/10.1016/0378-4347\(94\)00072-7](https://doi.org/10.1016/0378-4347(94)00072-7).

- [36] W.-F. Wang, J.-L. Yang, Advances in screening enzyme inhibitors by capillary electrophoresis, *Electrophoresis* 40 (2019) 2075–2083. <https://doi.org/10.1002/elps.201900013>.

- [37] S. Gattu, C.L. Crihfield, G. Lu, L. Bwanali, L.M. Veltri, L.A. Holland, Advances in enzyme substrate analysis with capillary electrophoresis, *Methods* 146 (2018) 93–106. <https://doi.org/10.1016/j.ymeth.2018.02.005>.

- [38] G.K.E. Scriba, F. Belal, Advances in capillary electrophoresis-based enzyme assays, *Chromatographia* 78 (2015) 947–970. <https://doi.org/10.1007/s10337-015-2912-0>.

- [39] B. Lindshield, Lipid digestion in the small intestine, in: *Intermed. Nutr.*, New Prairie Press, Manhattan, 2018: pp. 443–445. <https://newprairiepress.org/ebooks/19>.

- [40] B. Andualema, A. Gessesse, Microbial lipases and their industrial applications, *Biotechnol.* 11 (2012) 100–118. <https://doi.org/10.3923/biotech.2012.100.118>.

- [41] R. Sindhu, S. Shiburaj, A. Sabu, P. Fernandes, R. Singhal, G. Marina, I.C. Nair, K. Jayachandran, J. Vidya, L.P. de S. Vandenberghe, I. Deniz, A. Madhavan, P. Binod, R.K. Sukumaran, S.S. Kumar, M. Anusree, N. Nagavekar, M. Soumya, A. Jayakumar, E.K. Radhakrishnan, S.G. Karp, M. Giovana, M.G.B. Pagnoncelli, G.V. de M. Pereira, C.R. Soccol, S. Dogan, A. Pandey, Enzyme technology in food processing : recent developments and future prospects, in: *Innov. Food Process. Technol. A Compr. Rev.*, Elsevier, Amsterdam, ND, 2021: pp. 191–215. <https://doi.org/10.1016/B978-0-12-815781-7.00016-0>.

- [42] N.B. Melani, E.B. Tambourgi, E. Silveira, Lipases : from production to applications, *Sep. Purif. Rev.* 49 (2020) 143–158. <https://doi.org/10.1080/15422119.2018.1564328>.

- [43] N. Sarmah, D. Revathi, G. Sheelu, K.Y. Rani, S. Sridhar, V. Mehtab, C. Sumana, Recent advances on sources and industrial applications of lipases, *Biotechnol.* 34 (2018) 5–28. <https://doi.org/10.1002/btpr.2581>.

- [44] A. Houde, A. Kademi, D. Leblanc, Lipases and their industrial applications: an overview, *Appl. Biochem. Biotechnol.* 118 (2004) 155–170. <https://doi.org/10.1385/abab:118:1-3:155>.

- [45] F.I. Khan, D. Lan, R. Durrani, W. Huan, Z. Zhao, Y. Wang, The lid domain in lipases: structural and functional determinant of enzymatic properties, *Front. Bioeng. Biotechnol.* 5

- (2017) 1–1 3.
<https://doi.org/10.3389/fbioe.2017.00016>.
- [46] T. Zisis, P.L. Freddolino, P. Turunen, M.C.F. Van Teeseling, A.E. Rowan, K.G. Blank, Interfacial activation of *Candida antarctica* lipase B: combined evidence from experiment and simulation, *Biochemistry*. 54 (2015) 5969–5979.
<https://doi.org/10.1021/acs.biochem.5b00586>.
- [47] H. Bisswanger, Enzyme assays, *Perspect. Sci.* 1 (2014) 41–55.
<https://doi.org/10.1016/j.pisc.2014.02.005>.
- [48] J. Schejbal, G. Zdeněk, Immobilized-enzyme reactors integrated with capillary electrophoresis for pharmaceutical research, *J. Sep. Sci.* 41 (2018) 323–335.
<https://doi.org/10.1002/jssc.201700905>.
- [49] S. Huang, P. Paul, P. Ramana, E. Adams, P. Augustijns, A. Van Schepdael, Advances in capillary electrophoretically mediated microanalysis for on-line enzymatic and derivatization reactions., *Electrophoresis*. 39 (2018) 97–110.
<https://doi.org/10.1002/elps.201700262>.
- [50] C.M. Ouimet, C.I. D’amico, R.T. Kennedy, Advances in capillary electrophoresis and the implications for drug discovery., *Expert Opin. Drug Discov.* 12 (2017) 213–224.
<https://doi.org/10.1080/17460441.2017.1268121>.
- [51] S.-Y. Shi, Y.-P. Zhang, X.-Y. Jiang, X.-Q. Chen, K.-L. Huang, H.-H. Zhou, X.-Y. Jiang, Coupling HPLC to on-line, post-column (bio)chemical assays for high-resolution screening of bioactive compounds from complex mixtures, *TrAC Trends Anal. Chem.* 28 (2009) 865–877.
<https://doi.org/https://doi.org/10.1016/j.trac.2009.03.009>.
- [52] A. De Simone, M. Naldi, M. Bartolini, L. Davani, V. Andrisano, Immobilized enzyme reactors: an overview of applications in drug discovery from 2008 to 2018, *Chromatographia*. 82 (2019) 425–441.
<https://doi.org/10.1007/s10337-018-3663-5>.
- [53] S.-M. Fang, H.-N. Wang, Z.-X. Zhao, W.-H. Wang, Immobilized enzyme reactors in HPLC and its application in inhibitor screening: A review, *J. Pharm. Anal.* 2 (2012) 83–89.
<https://doi.org/https://doi.org/10.1016/j.jpha.2011.12.002>.
- [54] C.J. Malherbe, D. De Beer, E. Joubert, Development of on-Line high performance liquid chromatography (HPLC)-biochemical detection methods as tools in the identification of bioactives, *Int. J. Mol. Sci.* 13 (2012) 3101–3133.
<https://doi.org/10.3390/ijms13033101>.
- [55] J.S. Hill, R.C. Davis, D. Yang, J. Wen, J.S. Philo, P.H. Poon, M.L. Phillips, E.S. Kempner, H. Wong, Human hepatic lipase subunit structure determination, *J. Biol. Chem.* 271 (1996) 22931–22936.
<https://doi.org/10.1074/jbc.271.37.22931>.
- [56] U. Bornscheuer, O.W. Reif, R. Lausch, R. Freitag, T. Scheper, F.N. Kolisits, U. Menge, Lipase of *Pseudomonas cepacia* for biotechnological purposes: purification, crystallization

- and characterization, *Biochim. Biophys. Acta.* 1201 (1994) 55–60.
[https://doi.org/10.1016/0304-4165\(94\)90151-1](https://doi.org/10.1016/0304-4165(94)90151-1).
- [57] B. Vallejo-Cordoba, M.A. Mazorra-Manzano, A.F. González-Córdova, Determination of short-chain free fatty acids in lipolyzed milk fat by capillary electrophoresis., *J. Capill. Electrophor.* 5 (1998) 111–114.
- [58] L. Szente, J. Szejtli, J. Szemán, L. Kató, Fatty acid-cyclodextrin complexes: Properties and applications, *J. Incl. Phenom. Macrocycl. Chem.* 16 (1993) 339–354.
<https://doi.org/10.1007/BF00708714>.
- [59] G. Amores, M. Virto, Total and free fatty acids analysis in milk and dairy fat, *Separations.* 6 (2019) 1–22.
<https://doi.org/10.3390/separations6010014>.
- [60] M. Lubary, G.W. Hofland, J.H. ter Horst, The potential of milk fat for the synthesis of valuable derivatives, *Eur. Food Res. Technol.* 232 (2011) 1–8.
<https://doi.org/10.1007/s00217-010-1387-3>.
- [61] G. Hao, L. Yang, I. Mazsaroff, M. Lin, Quantitative determination of lipase activity by liquid chromatography-mass spectrometry, *J. Am. Soc. Mass. Spectr.* 18 (2007) 1579–1581.
<https://doi.org/10.1016/j.jasms.2007.05.019>.
- [62] T. Koseki, S. Asai, N. Saito, M. Mori, Y. Sakaguchi, K. Ikeda, Y. Shiono, Characterization of a novel lipolytic enzyme from *Aspergillus oryzae*, *Appl. Microbiol. Biotechnol.* 97 (2013) 5351–5357.
<https://doi.org/10.1007/s00253-012-4391-7>.
- [63] X. Chen, S. Xue, Y. Lin, J. Luo, L. Kong, Immobilization of porcine pancreatic lipase onto a metal-organic framework, PPL@MOF: A new platform for efficient ligand discovery from natural herbs, *Anal. Chim. Acta.* 1099 (2020) 94–102.
<https://doi.org/10.1016/j.aca.2019.11.042>.
- [64] J. Iqbal, S. Iqbal, C.E. Müller, Advances in immobilized enzyme microbioreactors in capillary electrophoresis, *Analyst.* 138 (2013) 3104–3116.
<https://doi.org/10.1039/c3an00031a>.
- [65] U. Guzik, K. Hupert-kocurek, D. Wojcieszynska, Immobilization as a strategy for improving enzyme properties-Application to oxidoreductases, *Molecules.* 19 (2014) 8995–9018.
<https://doi.org/10.3390/molecules19078995>.
- [66] Y. Tang, W. Li, Y. Wang, Y. Zhang, Y. Ji, Rapid on-line system for preliminary screening of lipase inhibitors from natural products by integrating capillary electrophoresis with immobilized enzyme microreactor, *J. Sep. Sci.* 43 (2019) 1003–1010.
<https://doi.org/10.1002/jssc.201900523>.
- [67] S. Kollipara, G. Bende, A.Á. Ema, Á. Regulatory, International guidelines for bioanalytical method validation : A comparison and discussion on current scenario, *Chromatographia.* 73 (2011) 201–217.
<https://doi.org/10.1007/s10337-010-1869-2>.

- [68] J. Liu, R.-T. Ma, Y.-P. Shi, An immobilization enzyme for screening lipase inhibitors from Tibetan medicines, *J. Chromatogr. A.* 1615 (2020) 1–8.
<https://doi.org/10.1016/j.chroma.2019.460711>.
- [69] C. Ruiz, S. Falcocchio, E. Xoxi, L. Villo, G. Nicolosi, F.I.J. Pastor, P. Diaz, L. Saso, Inhibition of *Candida rugosa* lipase by saponins, flavonoids and alkaloids, *J. Mol. Catal. B Enzym.* 40 (2006) 138–143.
<https://doi.org/10.1016/j.molcatb.2006.02.012>.
- [70] Y. Zhu, X. Ren, Y. Liu, Y. Wei, L. Qing, X. Liao, Covalent immobilization of porcine pancreatic lipase on carboxyl-activated magnetic nanoparticles: Characterization and application for enzymatic inhibition assays, *Mater. Sci. Eng. C.* 38 (2014) 278–285.
<https://doi.org/10.1016/j.msec.2014.02.011>.
- [71] G. Al Hamoui Dit Banni, R. Nasreddine, S. Fayad, P.C. Ngoc, J.C. Rossi, L. Leclercq, H. Cottet, A. Marchal, R. Nehmé, Screening for pancreatic lipase natural modulators by capillary electrophoresis hyphenated to spectrophotometric and conductometric dual detection, *Analyst.* 146 (2021) 1386–1401.
<https://doi.org/10.1039/D0AN02234A>.
- [72] S. Bernardo-Bermejo, E. Sánchez-López, M. Castro-Puyana, M.L. Marina, Chiral capillary electrophoresis, *Trends Anal. Chem.* 124 (2020) 1–18.
<https://doi.org/10.1016/j.trac.2020.115807>.
- [73] K.K. Bhardwaj, R. Gupta, Synthesis of chirally pure enantiomers by lipase, *J. Oleo Sci.* 66 (2017) 1073–1084.
<https://doi.org/10.5650/jos.ess17114>.
- [74] K. Pomeisl, N. Lamatová, V. Šolínová, R. Pohl, J. Brabcová, V. Kašíčka, M. Krečmerová, Enantioselective resolution of side-chain modified gem-difluorinated alcohols catalysed by *Candida antarctica* lipase B and monitored by capillary electrophoresis, *Bioorganic Med. Chem.* 27 (2019) 1246–1253.
<https://doi.org/10.1016/j.bmc.2019.02.022>.
- [75] A. Schuchert-Shi, P. C. Hauser, Following the lipase catalyzed enantioselective hydrolysis of amino acid esters with capillary electrophoresis using contactless conductivity detection, *Chirality.* 22 (2010) 331–335.
<https://doi.org/10.1002/chir.20746>.
- [76] B. Chankvetadze, W. Linder, G.K.E. Schriba, Enantiomer separations in capillary electrophoresis in the case of equal binding constants of the enantiomers with a chiral selector: Commentary on the feasibility of the concept, *Anal. Chem.* 76 (2004) 4256–4260.
<https://doi.org/10.1021/ac0355202>.
- [77] Y. Choi, J.-Y. Park, P.-S. Chang, Integral stereoselectivity of lipase based on the chromatographic resolution of enantiomeric/regioisomeric diacylglycerols, *J. Agric. Food Chem.* 69 (2021) 325–331.
<https://doi.org/10.1021/acs.jafc.0c07430>.
- [78] C. West, Recent trends in chiral supercritical fluid chromatography, *Trends Anal. Chem.*

- 120 (2019) 1–9.
<https://doi.org/10.1016/j.trac.2019.115648>.
- [79] A. Kumar, K. Dhar, S.S. Kanwar, P.K. Arora, Lipase catalysis in organic solvents: advantages and applications, *Biol. Proced. Online.* 18 (2016) 1–11.
<https://doi.org/10.1186/s12575-016-0033-2>.
- [80] W.L. Liu, N.S. Yang, Y.T. Chen, S. Lirio, C.Y. Wu, C.H. Lin, H.Y. Huang, Lipase-supported metal-organic framework bioreactor catalyzes warfarin synthesis, *Chem. Eur. J.* 21 (2015) 115–119.
<https://doi.org/10.1002/chem.201405252>.
- [81] S.F.Y. Li, L.J. Kricka, Clinical analysis by microchip capillary electrophoresis, *Clin. Chem.* 52 (2006) 37–45.
<https://doi.org/10.1373/clinchem.2005.059600>.
- [82] I. Hamdan I., H. Zalloum, Pancreatic lipase inhibitory activity of selected pharmaceutical agents, *Acta Pharm.* 69 (2019) 1–16.
- [83] C.J. Wienken, P. Baaske, U. Rothbauer, D. Braun, S. Duhr, Protein-binding assays in biological liquids using microscale thermophoresis, *Nat. Commun.* 1 (2010) 1–7.
<https://doi.org/10.1038/ncomms1093>.
- [84] M. Jerabek-Willemsen, C.J. Wienken, D. Braun, P. Baaske, S. Duhr, Molecular interaction studies using microscale thermophoresis, *Assay Drug Dev. Technol.* 9 (2011) 342–353.
<https://doi.org/10.1089/adt.2011.0380>.
- [85] M. Jerabek-Willemsen, T. André, R. Wanner, H.M. Roth, S. Duhr, P. Baaske, D. Breitsprecher, Microscale thermophoresis: interaction analysis and beyond, *J. Mol. Struct.* 1077 (2014) 101–113.
<https://doi.org/10.1016/j.molstruc.2014.03.009>.
- [86] H. Mazal, H. Aviram, I. Riven, G. Haran, Effect of ligand binding on a protein with a complex folding landscape, *Phys. Chem. Chem. Phys.* 20 (2018) 3054–3062.
<https://doi.org/10.1039/c7cp03327c>.
- [87] S. Priet, L. Roux, M. Saez-Ayala, F. Ferron, B. Canard, K. Alvarez, Enzymatic synthesis of acyclic nucleoside thiophosphonate diphosphates: Effect of the α -phosphorus configuration on HIV-1 RT activity, *Antivir. Res.* 117 (2015) 122–131.
<https://doi.org/10.1016/j.antiviral.2015.03.003>.
- [88] F. Syntia, R. Nehmé, B. Claude, P. Morin, Human neutrophil elastase inhibition studied by capillary electrophoresis with laser induced fluorescence detection and microscale thermophoresis, *J. Chromatogr. A.* 1431 (2016) 215–223.
<https://doi.org/10.1016/j.chroma.2015.12.079>.
- [89] G. Al Hamoui Dit Banni, R. Nasreddine, S. Fayad, C. Colas, A. Marchal, R. Nehmé, Investigation of lipase-ligand interactions in porcine pancreatic extracts by microscale thermophoresis, *Anal. Bioanal. Chem.* 413 (2021) 3667–3681.
<https://doi.org/10.1007/s00216-021-03314-7>.
- [90] D. Deville-bonne, C. El, P. Meyer, Y. Chen, L.A. Agrofoglio, J. Janin, Human and viral

- 997 nucleoside/nucleotide kinases involved in antiviral drug activation: structural and catalytic
 998 properties, *Antivir. Res.* 86 (2010) 101–120.
 999 <https://doi.org/10.1016/j.antiviral.2010.02.001>.
- 1000 [91] S. Banditelli, C. Baiocchi-ii, R. Pesi, S. Allegrini, M. Turriani, P.L. Ipata, M.C.A.M. Ici,
 1001 M.G. Tozzi, The phosphotransferase activity of cytosolic 5'-nucleotidase ; a purine analog
 1002 phosphorylating enzyme, *Int. J. Biochem. Cell Biol.* 28 (1996) 711–720.
 1003 [https://doi.org/https://doi.org/10.1016/1357-2725\(95\)00171-9](https://doi.org/https://doi.org/10.1016/1357-2725(95)00171-9).
- 1004 [92] H. Tzeng, H. Hung, Simultaneous determination of thymidylate and thymidine diphosphate
 1005 by capillary electrophoresis as a rapid monitoring tool for thymidine kinase and thymidylate
 1006 kinase activities, *Electrophoresis.* 26 (2005) 2225–2230.
 1007 <https://doi.org/10.1002/elps.200410091>.
- 1008 [93] T. Drevinskas, L. Telksnys, A. Maruška, J. Gorbatsova, M. Kaljurand, Capillary
 1009 electrophoresis sensitivity enhancement based on adaptive moving average method, *Anal.*
 1010 *Chem.* 90 (2018) 6773–6780.
 1011 <https://doi.org/10.1021/acs.analchem.8b00664>.
- 1012 [94] C.C. Liu, J.S. Huang, D.L.J. Tyrrell, N.J. Dovichi, Capillary electrophoresis-electrospray-
 1013 mass spectrometry of nucleosides and nucleotides: Application to phosphorylation studies
 1014 of anti-human immunodeficiency virus nucleosides in a human hepatoma cell line,
 1015 *Electrophoresis.* 26 (2005) 1424–1431.
 1016 <https://doi.org/10.1002/elps.200410423>.
- 1017 [95] J. Iqbal, B. Joachim C, M. Christa E, Development of off-line and on-line capillary
 1018 electrophoresis methods for the screening and characterization of adenosine kinase
 1019 inhibitors and substrates, *Electrophoresis.* 27 (2006) 2505–2517.
 1020 <https://doi.org/10.1002/elps.200500944>.
- 1021 [96] R. Nehmé, C. Perrin, V. Guerlavais, J.A. Fehrentz, H. Cottet, J. Martinez, H. Fabre, Use of
 1022 coated capillaries for the electrophoretic separation of stereoisomers of a growth hormone
 1023 secretagogue, *Electrophoresis.* 30 (2009) 3772–3779.
 1024 <https://doi.org/10.1002/elps.200900093>.
- 1025 [97] J. Iqbal, L. Scapozza, G. Folkers, E.M. Christa, Development and validation of a capillary
 1026 electrophoresis method for the characterization of herpes simplex virus type 1 (HSV-1)
 1027 thymidine kinase substrates and inhibitors, *J. Chromatogr. B.* 846 (2007) 281–290.
 1028 <https://doi.org/10.1016/j.jchromb.2006.09.018>.
- 1029 [98] J. Ferey, D. Da Silva, C. Colas, R. Nehmé, P. Lafite, V. Roy, P. Morin, R. Daniellou, L.
 1030 Agrofoglio, B. Maunit, Monitoring of successive phosphorylations of thymidine using free
 1031 and immobilized human nucleoside / nucleotide kinases by Flow Injection Analysis with
 1032 High-Resolution Mass Spectrometry, *Anal. Chim. Acta.* 1049 (2019) 115–122.
 1033 <https://doi.org/10.1016/j.aca.2018.10.032>.
- 1034 [99] R. Roskoski, Michaelis-Menten kinetics, in: *Ref. Modul. Biomed. Sci.*, Elsevier, 2015.
 1035 <https://doi.org/https://doi.org/10.1016/B978-0-12-801238-3.05143-6>.
- 1036 [100] H. Whately, Basic principles and modes of capillary electrophoresis, in: J. Petersen, A.A.

- Mohammad (Eds.), Clin. Forensic Appl. Capill. Electrophor., Humana Press, New Jersey, 2001: pp. 21–58.
<https://doi.org/10.1007/978-1-59259-120-6>.
- [101] D.N. Heiger, High performance capillary electrophoresis: an introduction: a primer, Agilent Technologies, Germany, 2000. <https://books.google.fr/books?id=6KGJjgEACAAJ>.
- [102] N. Malartre, R. Boulieu, N. Falah, J.C. Cortay, B. Lina, F. Morfin, E. Frobert, Effects of mutations on herpes simplex virus 1 thymidine kinase functionality: an in vitro assay based on detection of monophosphate forms of acyclovir and thymidine using HPLC/DAD, Antivir. Res. 95 (2012) 224–228. <https://doi.org/10.1016/j.antiviral.2012.07.001>.
- [103] C. Machon, F. Catez, N.D. Venezia, F. Vanhalle, L. Guyot, A. Vincent, M. Garcia, B. Roy, J.J. Diaz, J. Guitton, Intracellular anabolism of 5-fluorouracil and incorporation in nucleic acids based on an LC-HRMS method, J. Pharm. Anal. 11 (2021) 77–87. <https://doi.org/https://doi.org/10.1016/j.jpha.2020.04.001>.
- [104] S. Bustamante, R.B. Gilchrist, D. Richani, A sensitive method for the separation and quantification of low-level adenine nucleotides using porous graphitic carbon-based liquid chromatography and tandem mass spectrometry, J. Chromatogr. B. 1061–1062 (2017) 445–451. <https://doi.org/10.1016/j.jchromb.2017.07.044>.
- [105] J. V Pagaduan, M. Ramsden, K.O. Neill, A.T. Woolley, Microchip immunoaffinity electrophoresis of antibody – thymidine kinase 1 complex, Electrophoresis. 36 (2015) 813–817. <https://doi.org/10.1002/elps.201400436>.

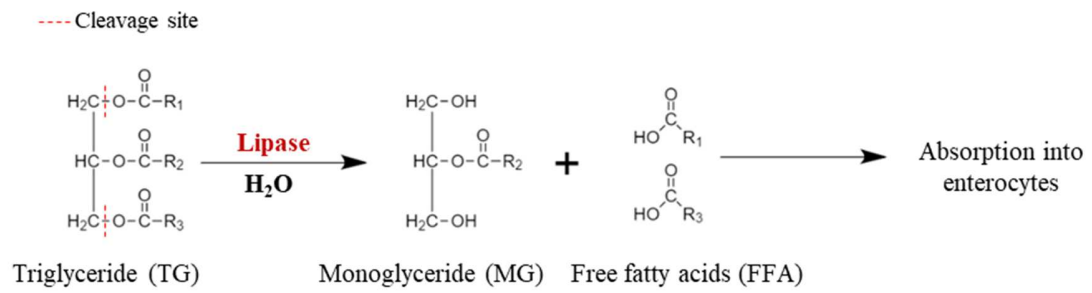


Figure 1: An illustration of TG hydrolysis catalyzed by lipases

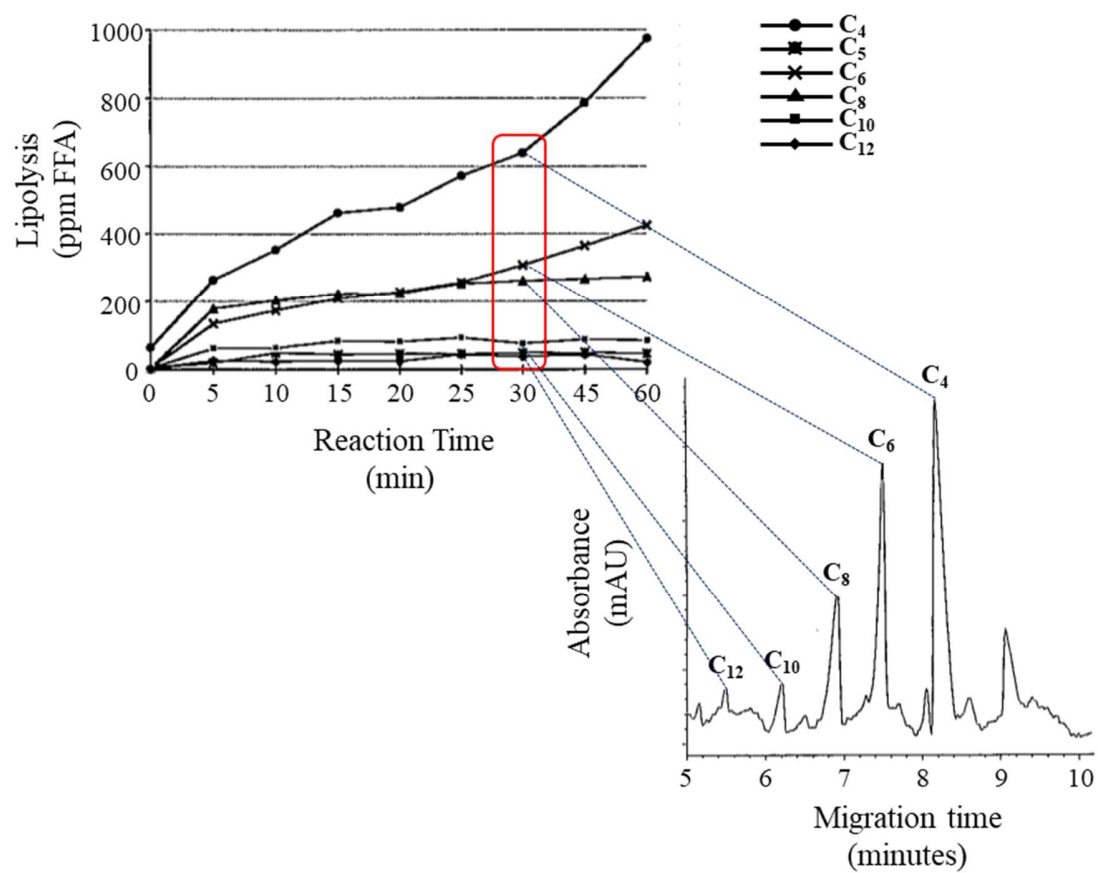


Figure 2: Kinetics of lipase catalyzed hydrolysis of cream fat into FFA (a) and, electropherogram of FFA in lyophilized cream for 30 min (b). Adapted from [57]. Reaction and separation conditions are summarized in Table 1

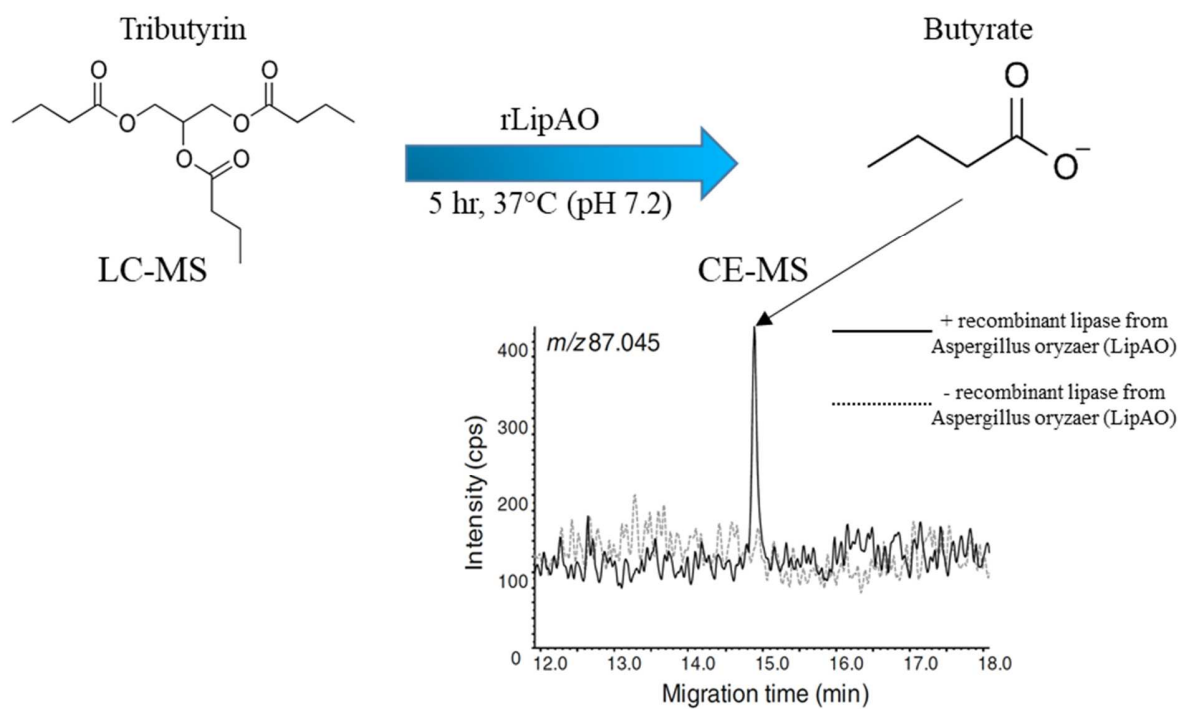
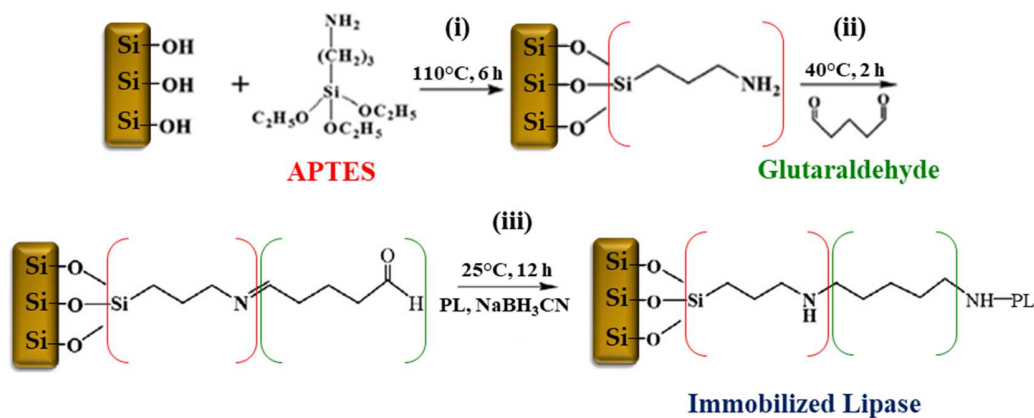
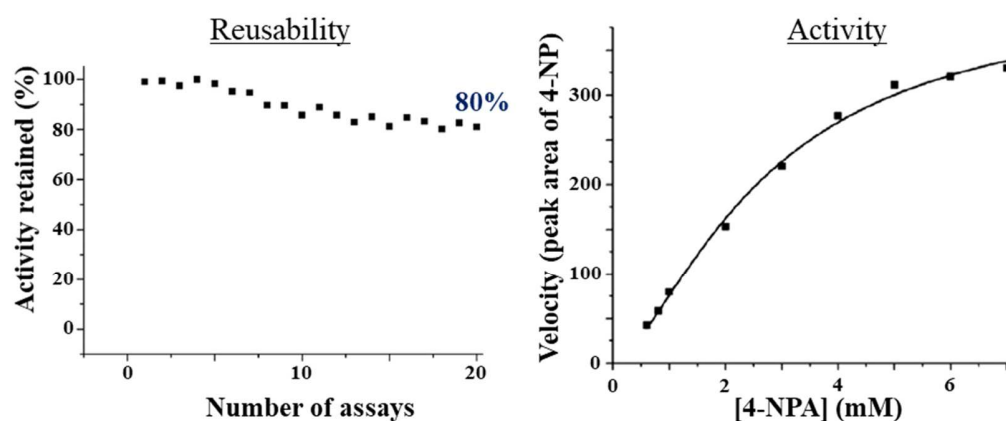


Figure 3: Hydrolysis of tributyrin by rLipAO from *Aspergillus oryzae* into butyrate detected by CE-TOF-MS as depicted in the electropherogram. The tributyrin substrate was monitored using LC-(Q-TOF-MS). Conditions of the enzymatic reaction, LC-MS and CE-MS are summarized in Table 1. Adapted from [62]

(a) PL immobilization *via* cross-linking



(b) Characterization of immobilized PL



(c) Inhibitor screening

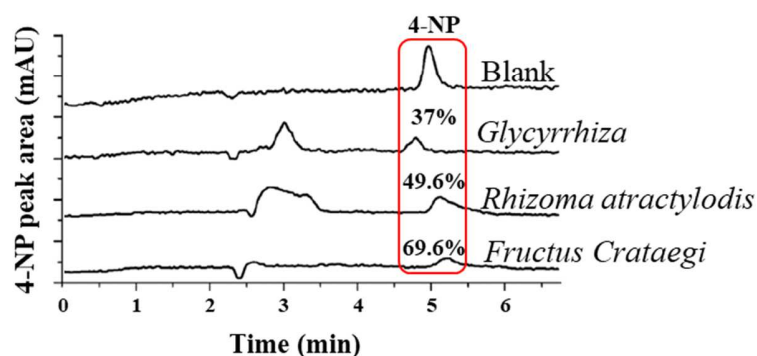


Figure 4: Illustration of PL immobilization onto the capillary wall *via* cross-linking using glutaraldehyde as a bifunctional linker (a), Immobilized PL reusability over 20 assays and activity over a range of 4-NPB concentrations (0.6-7 mM) (b) and, Screening of plant extracts at 10 mg mL^{-1} for PL inhibition (c). More conditions of enzymatic reaction, inhibition assays and CE separation are summarized in Table 1. Adapted from [66]

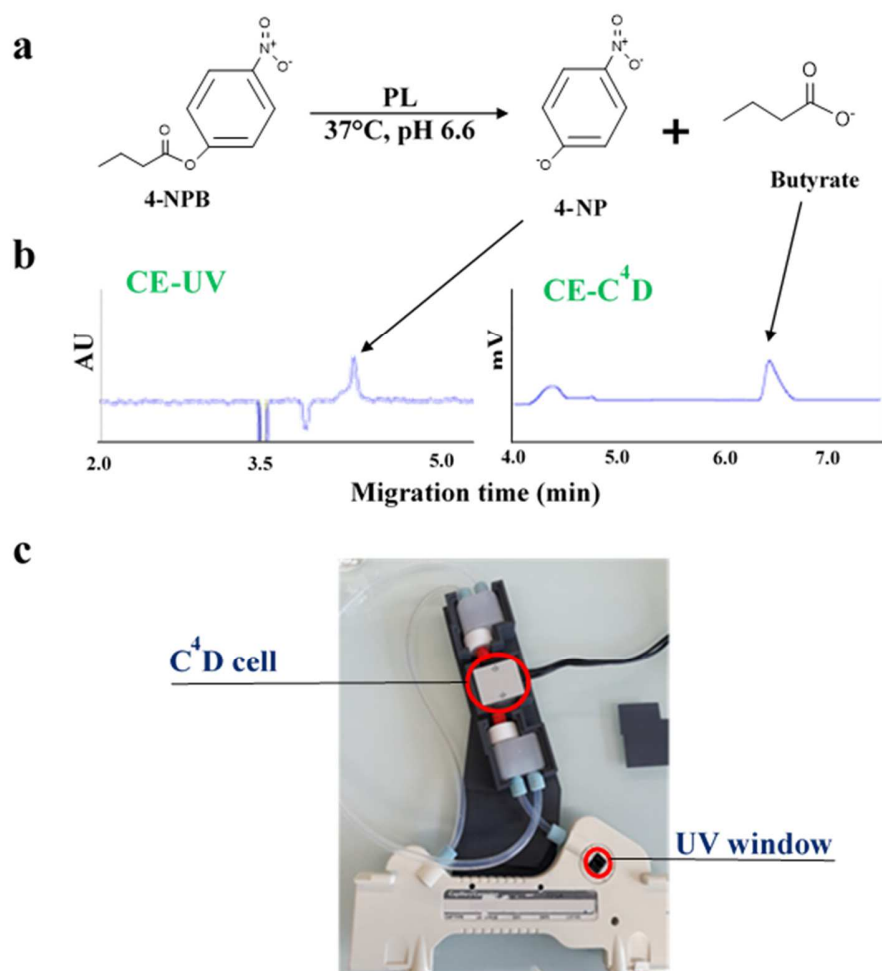


Figure 5: Lipase-catalyzed hydrolysis of 4-NPB into 4-NP and butyrate (a). Electropherograms for the detection of 4-NP and butyrate individually by CE-UV and CE-C⁴D, respectively (b). Demonstration of the dual detector cartridge with an adapted 3D-printed scaffold (c). Adapted from [71]

(1)-(18-crown-6)-2,3,11,12-tetracarboxylic acid

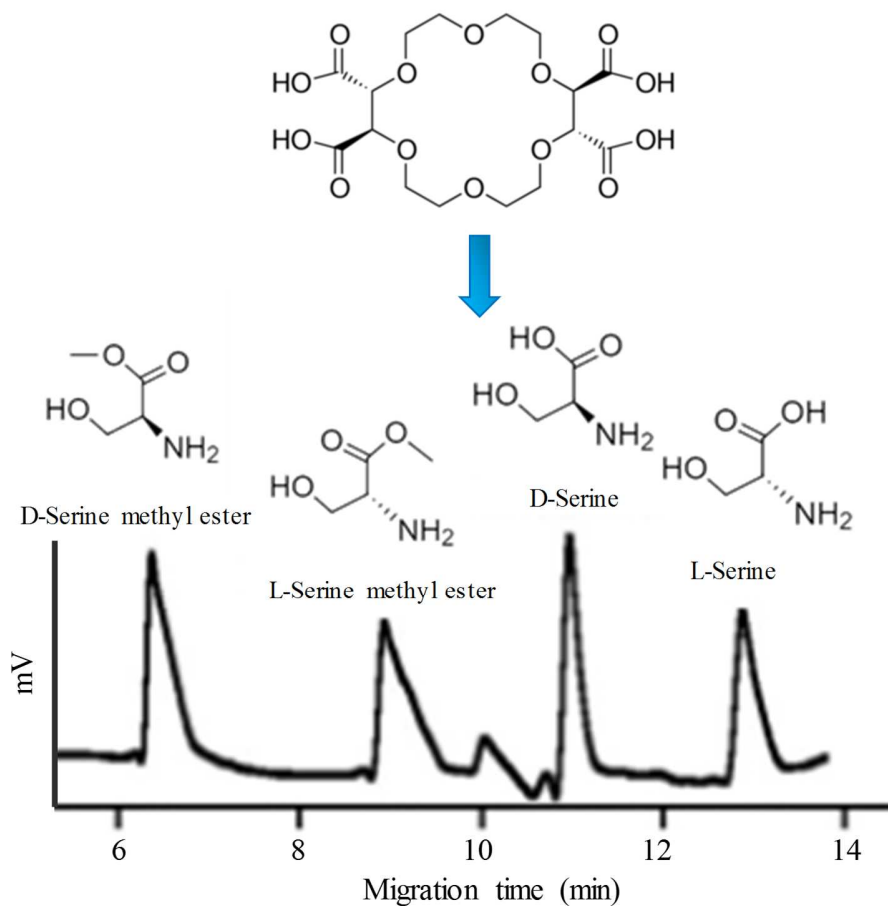


Figure 6: Electropherogram obtained for the separation of 5 mM D- and L-serine methyl esters as well as 5 mM D- and L-serine using (+)-(18-crown-6)-2,3,11,12-tetracarboxylic acid as a chiral selector and C^4D as detector. Adapted from [75]. Conditions summarized in Table 1

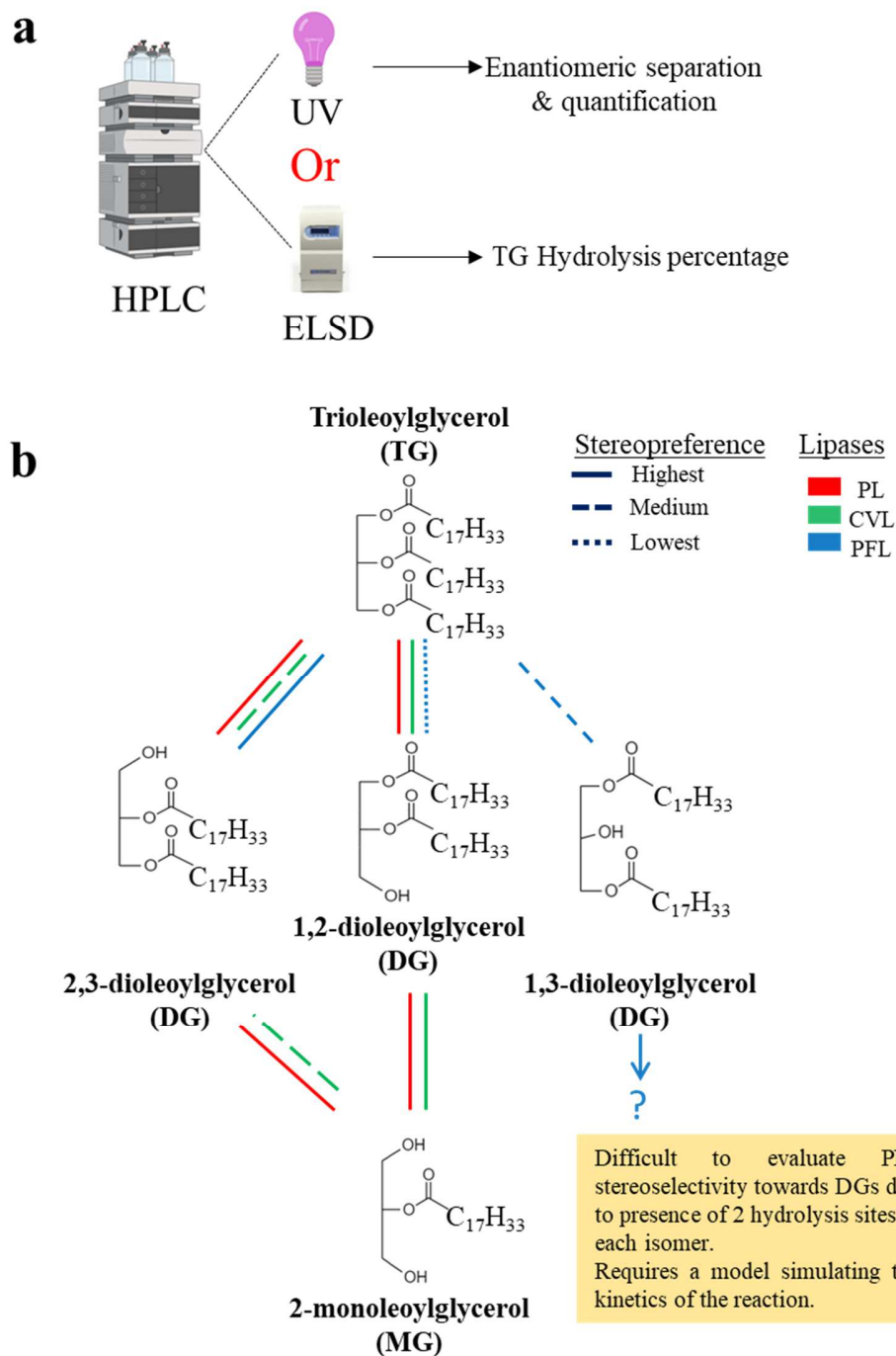
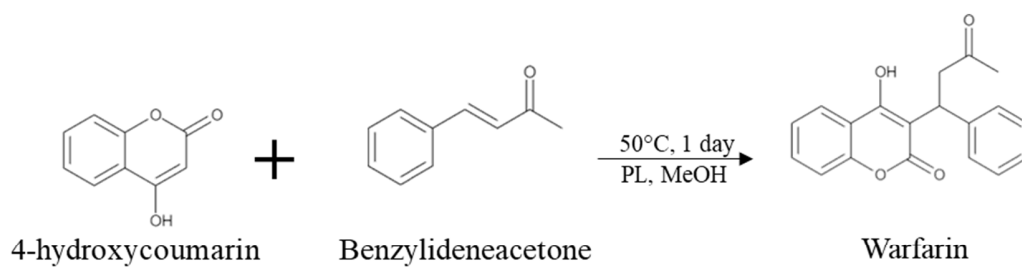


Figure 7: Quantification of enantiomeric isomers and determination of TG hydrolysis percentage by HPLC-UV and HPLC-ELSD, respectively (**a**) and, Stereoselectivity of three different lipases towards TG and DG enantiomers (**b**)

a



b

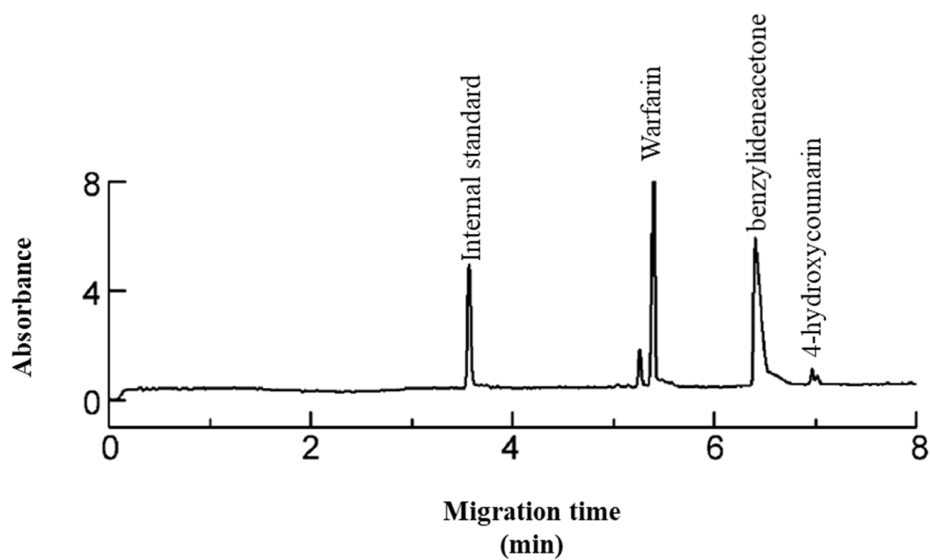
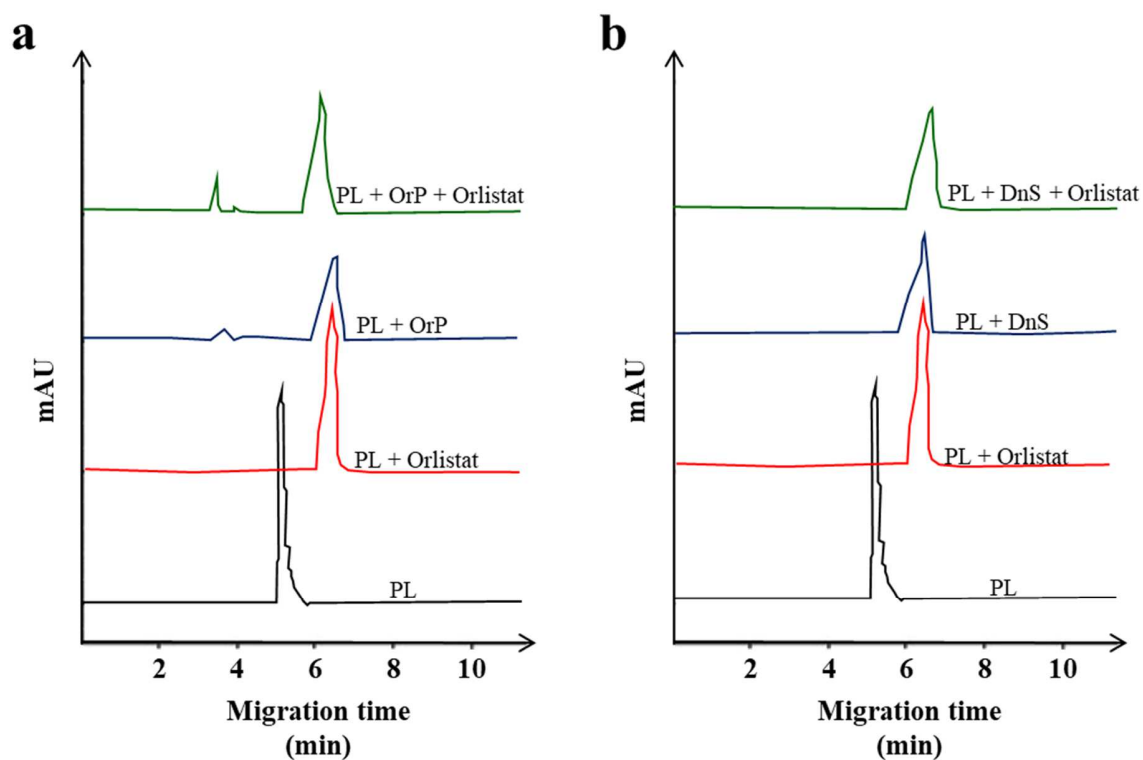


Figure 8: PL catalyzed reaction for warfarin synthesis from 4-hydroxycoumarin and benzylideneacetone (**a**) and, electropherogram of the PL-MOF reaction mixture analyzed by CE-UV at $\lambda = 214$ nm (**b**). Adapted from [80]. Reaction and CE conditions are summarized in Table 1



c Structures of PL inhibitor compounds

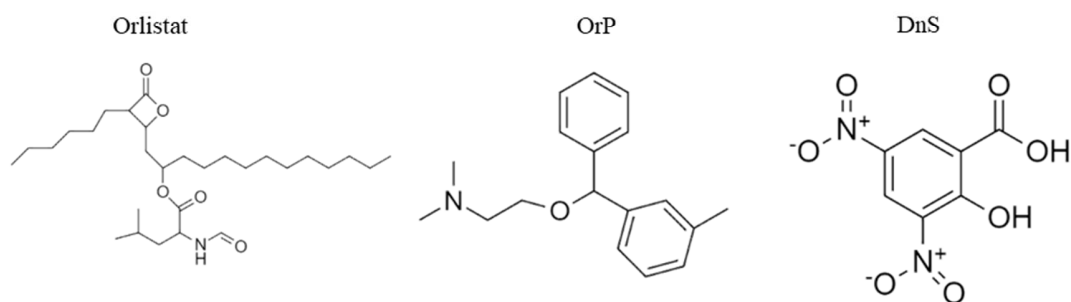


Figure 9: Electropherograms obtained for monitoring the shape of the PL peak. PL peak in the presence or absence of orlistat in addition to the presence of orphenadrine (OrP) and OrP + Orlistat (**a**) and, dinitrosalicylic acid (DnS) and DnS + Orlistat (**b**). The structures of the investigated PL inhibitory compounds are presented in (**c**). Adapted from [82]

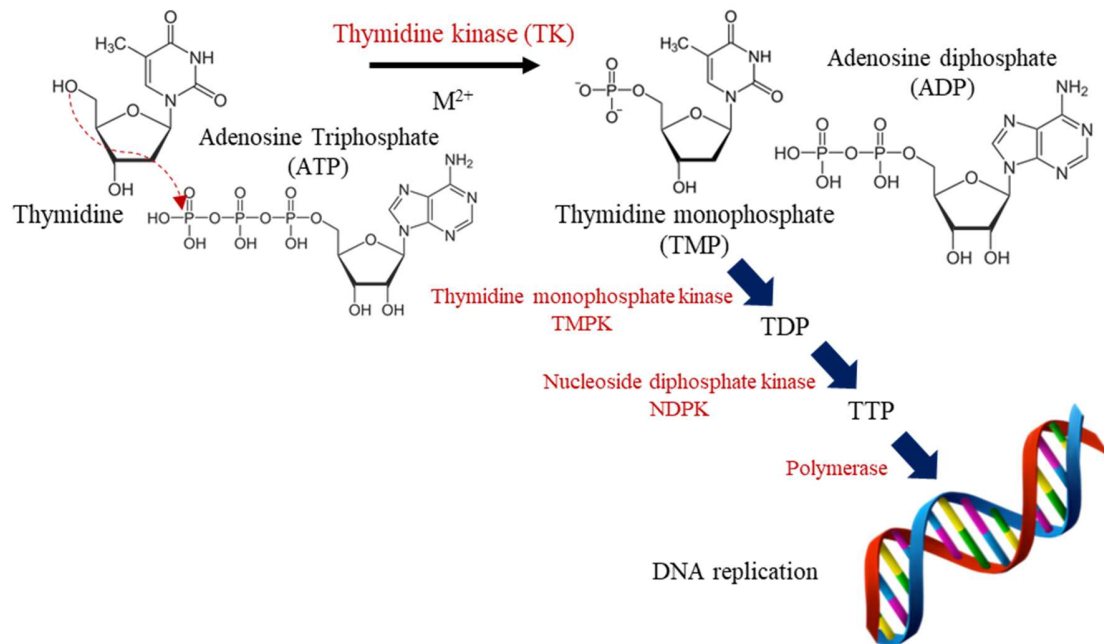


Figure 10: Illustration of the phosphorylation cascade leading to DNA replication and involving multiple kinases. M^{2+} : Divalent metal cation such as Mg^{2+} or Mn^{2+}

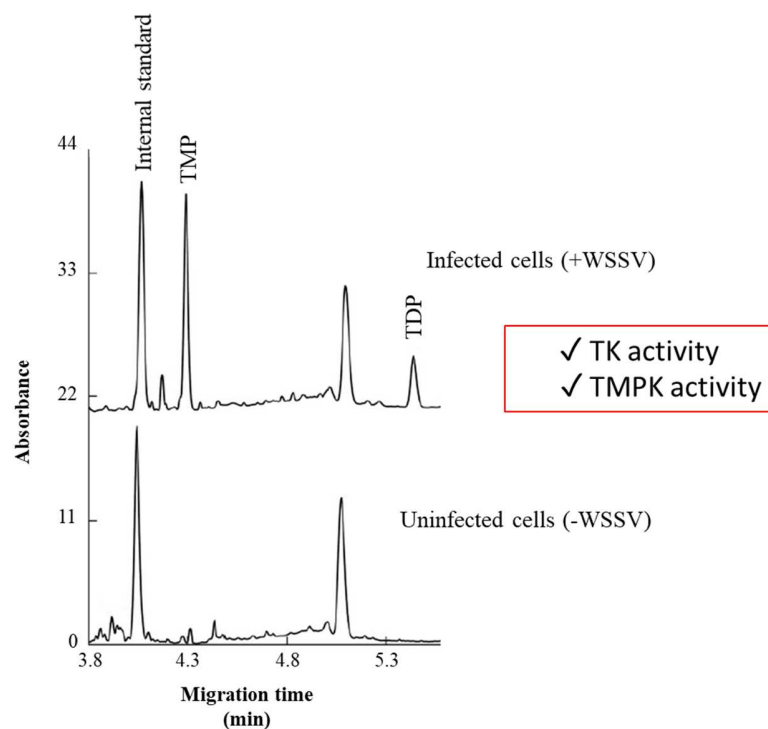


Figure 11: Electropherograms obtained for the detection of TMP and TDP from insect cell lines after infection with White spot syndrome virus (WSSV) indicating TK and TMPK activities of the virus, respectively. Adapted from [92]. Reaction and CE conditions are summarized in Table 2

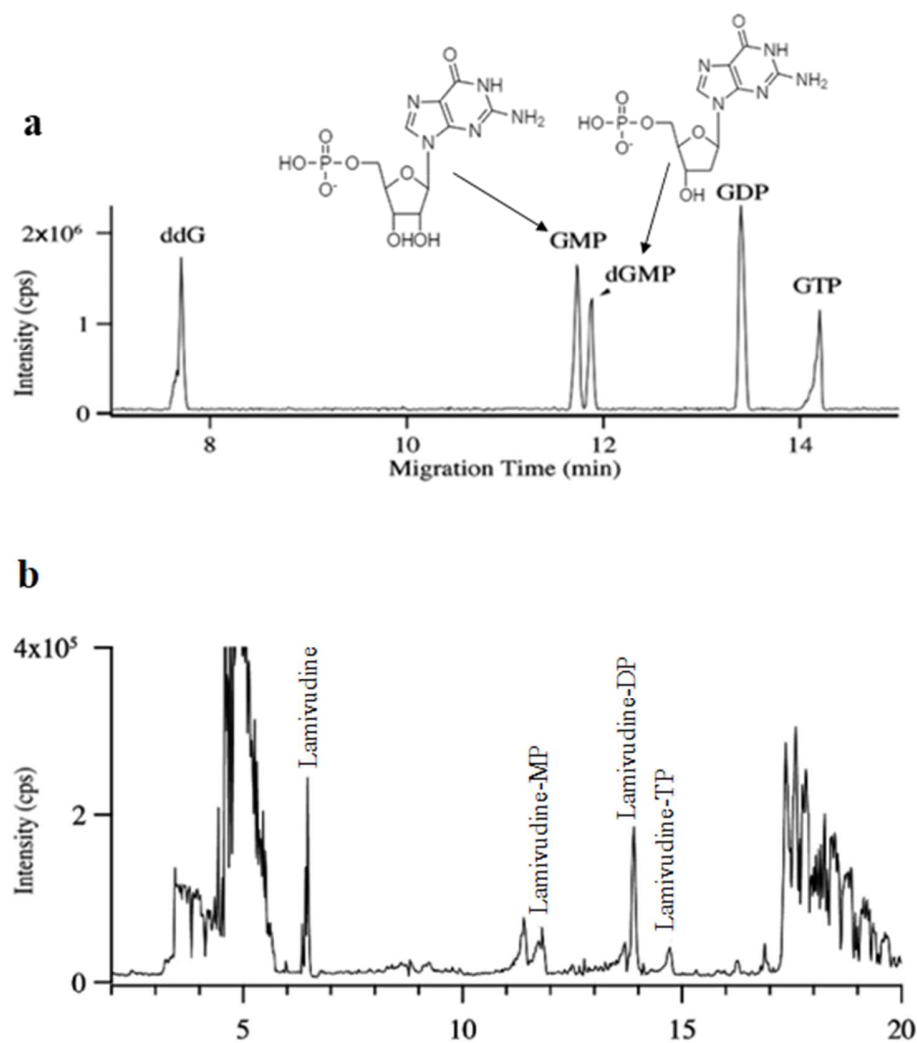


Figure 12: electropherogram representing the separation of various Guanosine nucleoside phosphates in addition to the resolution of dGMP from GMP (a) and, electropherogram of the CE-MS analysis of cell extracts incubated in lamivudine-containing medium demonstrating cellular phosphorylation activity (b). Reaction and CE-MS conditions are summarized in Table 2. Adapted from [94]

a

Method A	Substrate	% phosphorylation
Testing nucleoside substrates offline	Adenosine	100 ± 2
	2-Ethylaminoadenosine	3 ± 1
	2-Isopropylaminoadenosine	4 ± 0
	2-Isopropylamino-N6-isopropyladenosine	81 ± 3
	2-Benzylaminoadenosine	4 ± 0
	2-Cyclohexylaminoadenosine	3 ± 0
	2-(Pyrrolidin-1-yl)adenosine	53 ± 2
	2-(4-Benzylpiperazin-1-yl)adenosine	3 ± 0

b

Method B	K _i value (nM)			
Testing AK inhibitor offline		Offline CE-UV (Method B)	Online-CE-UV (Method C)	Radioactive method
	AK Inhibitor	Bovine AK		
	ABT-702	1.4 ± 0.04	1.7 ± 0.07	3.4 ± 0.03
Method C	5-IT	30.6 ± 1.7	n.d.	29 ± 6.1
Testing AK inhibitor online	A-134974	0.09 ± 0.006	0.06 ± 0.031	0.07 ± 0.006
				0.06 ± 0.07

Figure 13: The percentage phosphorylation obtained for 8 substrates of bovine AK using offline CE (a) and, K_i values obtained for 3 AK inhibitors using offline and online CE as well as a conventional radioactivity assay using bovine and human AK (b). Reaction and separation conditions for all three methods are summarized in Table 2

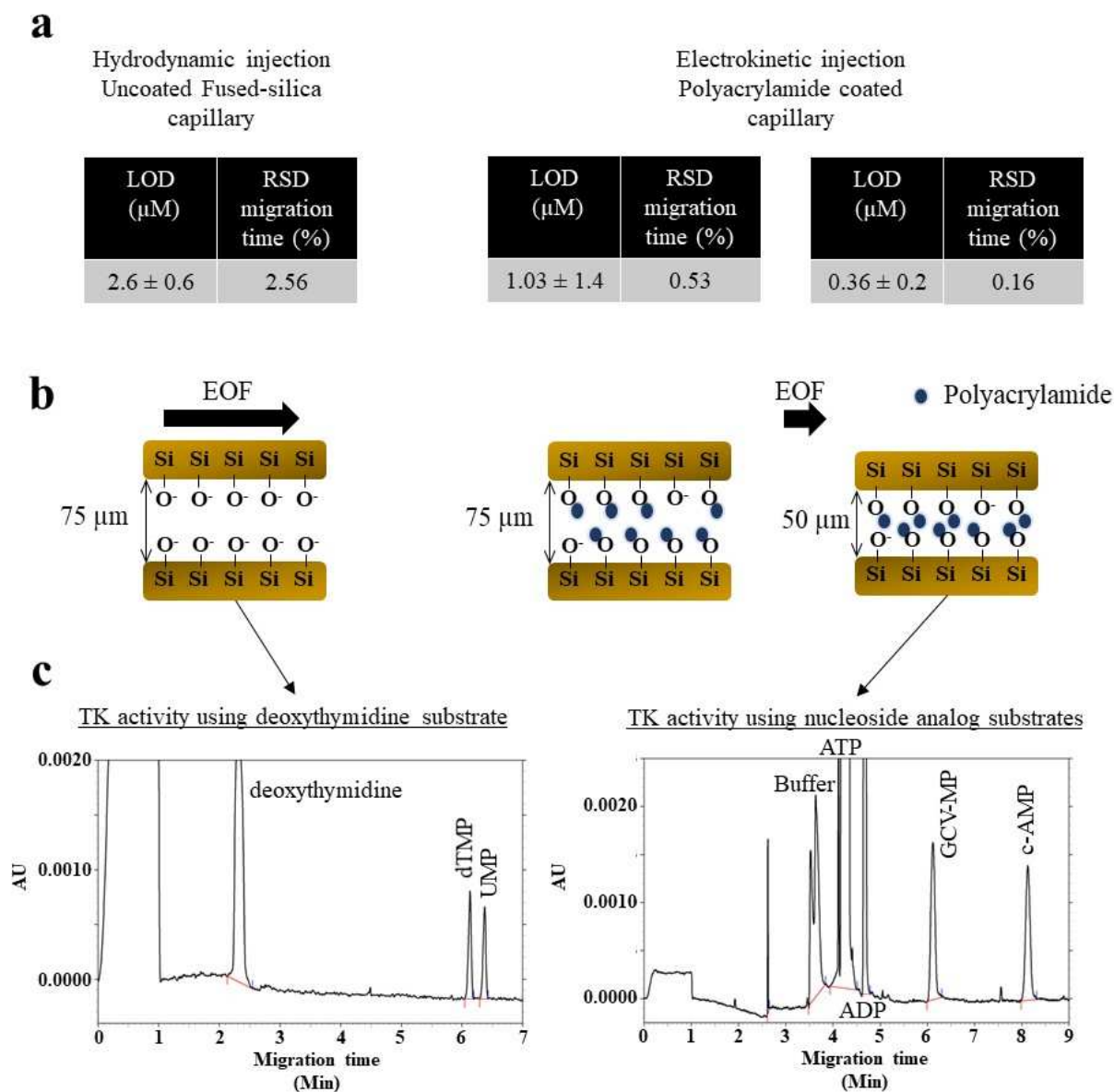


Figure 14: The LOD of mono-phosphorylated nucleoside or nucleoside analogs and the RSD of migration times between all three types of capillaries used (**a**), Illustration of the inner polyacrylamide-coated surface of the capillaries (**b**) and, electropherograms obtained by CE-UV for the phosphorylation of endogeneous deoxythymidine (left) and nucleoside analog GCV (right) (**c**). Conditions of enzymatic reaction and CE separation are summarized in Table 2. Electropherograms adapted from [97]

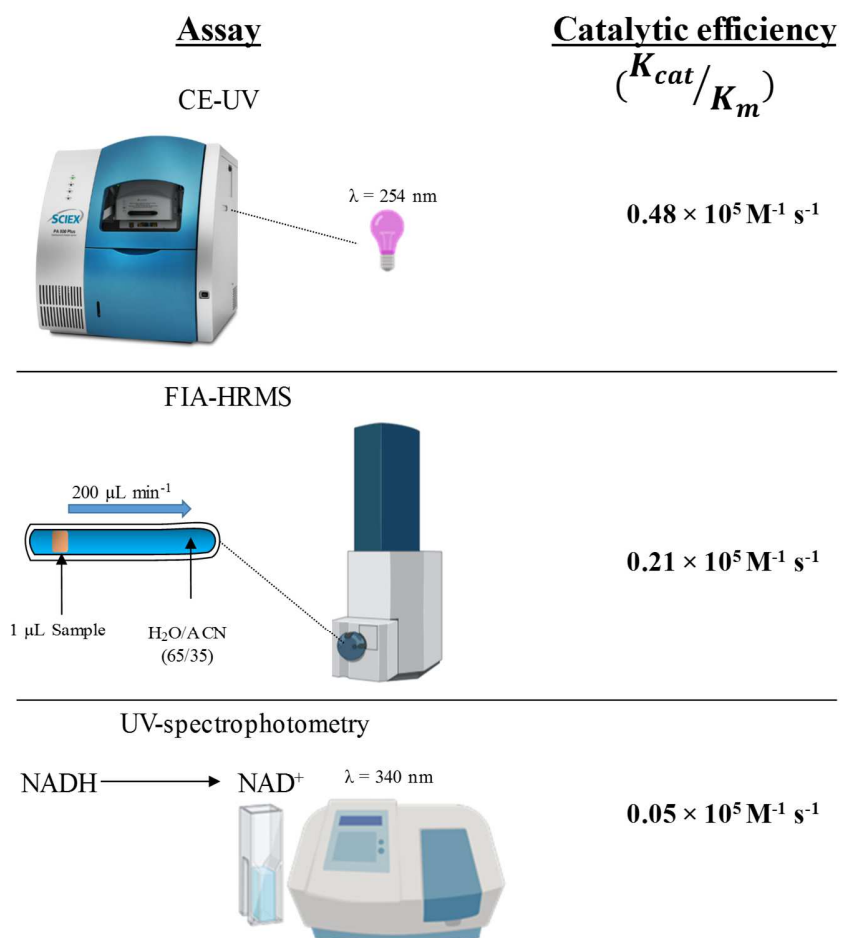


Figure 15: Catalytic efficiency of TMPK assayed by three different techniques (CE-UV, FIA-HRMS and UV spectrophotometry)

Table 1: CE-based lipase assays

Enzymatic reaction					CE separation		
	Enzyme	Substrate	Inhibitor	Incubation buffer (IB)	Reaction conditions	Background electrolyte (BGE)	CE conditions
[57]	Palastase 20000 L (Commercial lipase from <i>Rhizomucor miehei</i>)	Cream fat	-	Cream matrix, maintained at pH 7.0 through the addition of 0.1 N NaOH	<u>Offline reaction</u> Lipase added to 1000 g of cream Incubation at 40°C for 60 min with constant stirring Reaction mixture aliquoted at different time points (0-60 min). Reaction was stopped by boilingfor 5 min Aliquots were mixed with tris, p-ainsate and β-CD before CE injection	20 mM Tris 10 mM p-anisate 1 mM trimethyl β-CD (pH 8.0)	Uncoated fused-silica capillary: 80.5 cm × 50 μm i.d.; 72 cm effective length Temperature: 30°C Separation voltage: +30 kV Injection:0.7 psi × 10 s (11 nL) Detection: indirect UV FFA at λ = 270 nm
[62]	rLipAO (lipase from <i>Aspergillus oryzae</i> fungi)	Glycerol tributyrate Or tributyrin	-	50 mM MOPS/KOH 10 mM MgCl ₂ 10 mM KCl (pH 7.2)	<u>Offline reaction:</u> Lipase added to tributyrin in IB Incubation at 37°C for 1 and 5 h Aliquots were collected and diluted with MeOH	50 mM ammonium acetate (pH 8.5)	SMILE (+) coated capillary 120 cm × 50 μm i.d. Separation voltage: -30 kV Detection: ESI-MS Butyrate (<i>m/z</i> = 87.045) Sheath liquid: 5 mM ammonium acetate in

Enzymatic reaction					CE separation	
Enzyme	Substrate	Inhibitor	Incubation buffer (IB)	Reaction conditions	Background electrolyte (BGE)	CE conditions
				to stop the reaction The sample was filtered <i>via</i> ultrafiltration with a 5,000 Da cutoff before injection into LC- or CE-MS		50% (v/v) MeOH/H ₂ O Negative ionization mode Capillary voltage: 3.5 kV Dry gas: N ₂ at 10 psi
[66]	Porcine pancreatic lipase (PL), type II Covalently immobilized onto the capillary walls <i>via</i> cross-linking	4-nitrophenyl acetate (4-NPA) Ten ethanolic plant extracts (extracted by ultrasonic-assisted extraction) used in Chinese medicines	Orlistat 10 mM Na ₂ HPO ₄ (pH 8.0) adjusted with 1 M H ₃ PO ₄	<u>Immobilized enzyme microreactor (IMER)</u> Capillary rinsed with 10 mM Na ₂ HPO ₄ for 3 min 4-NPA with or without orlistat or plant extract injected at 0.7 psi × 5 sec; 64 nL Incubation at 25°C for 4 min Reaction was stopped by the application of the separation voltage	10 mM Na ₂ HPO ₄ (pH 8.0) adjusted with 1 M H ₃ PO ₄	APTES/GA activated (16.5 cm) and uncoated fused silica (16.5 cm) capillary connected by a 0.5 cm Teflon tubing 33 cm × 75 µm i.d.; 8.5 cm effective length Temperature: 25°C Separation voltage: +15kV Injection: 0.7 psi × 5 s (64 nL) Detection: UV 4-NP at λ = 400 nm
[68]	<i>Candida rugosa</i> lipase (CRL) immobilized onto Fe ₃ O ₄ @TiO ₂ NP by electrostatic interactions.	4-nitrophenyl palmitate (4-NPP) 6 methanolic plant extracts used in Tibetan medicine	Orlistat 20 mM NaH ₂ PO ₄ (pH 4 – 10)	<u>Offline reaction</u> 4-NPP added to a solution of immobilized CRL NP	20 mM Na ₂ B ₄ O ₇ ·10H ₂ O (pH 9.0) adjusted with 1 M HCl	Uncoated fused-silica capillary (33 cm × 50 µm i.d.; 24.5 cm effective length) Temperature: 20°C

Enzymatic reaction					CE separation	
Enzyme	Substrate	Inhibitor	Incubation buffer (IB)	Reaction conditions	Background electrolyte (BGE)	CE conditions
		11 compounds isolated from <i>Oxytropis falcate</i>		For inhibition assays, plant extracts or isolated compounds were added to the mixture Incubation at 60°C for 15 min Reaction was stopped by separating immobilized CRL NP using a magnet		Separation voltage: +20 kV Detection: UV 4-NP at $\lambda = 405$ nm
[71]	Porcine pancreatic lipase (PL)	4-nitrophenyl butyrate (4-NPB)	Orlistat 7 Aqueous extracts from 3 plants (1 mg mL ⁻¹) 11 molecules purified from oakwood or wine (1 mg mL ⁻¹)	10 mM Tris 40 mM MOPS (pH 6.6) <u>Offline reaction:</u> PL added to a solution containing: IB, Substrate Modulators (Inhibition assays) Incubation at 37°C for 5 min Reaction was stopped by boiling for 5 min Reaction mixture was centrifuged at 2000g for 5 min before CE analysis <u>Online reaction:</u> 1 st plug: PL + modulator	10 mM Tris + 40 mM MOPS (pH 6.6)	Uncoated fused-silica capillary (61 cm × 50 μ m i.d.; 37 cm effective length to C ⁴ D; 51 cm effective length to UV) Temperature: 37°C Separation voltage: +30 kV Injection (offline): 0.7 psi × 5 s; (9 nL) Detection: UV 4-NP at $\lambda = 400$ nm C ⁴ D Butyrate at frequency: medium, 0 dB voltage,

Enzymatic reaction					CE separation	
Enzyme	Substrate	Inhibitor	Incubation buffer (IB)	Reaction conditions	Background electrolyte (BGE)	CE conditions
				0.5 psi × 3 s (4 nL)		100% gain, 010 offset, 1/3 filter frequency and 0.02 filter cut-off
				2 nd plug: 4-NPB 0.5 psi × 6 s (8 nL)		
				3 rd plug: same as 1 st plug		
				4 th plug: IB 0.5 psi × 90 s (120 nL)		
				Incubation at 37°C for 5 min		
[74]	<i>Candida antartica</i> lipase B (CALB)	3-(benzyloxy)-1,1-difluoropropan-2-ol	-	Reaction was stopped as soon as the separation voltage was applied	22 mM NaOH + 35 mM H ₃ PO ₄ (pH 2.5) + 1.5 mM sulfobutyl ether β-cyclodextrin (β-CD)	Uncoated fused-silica capillary (40.6 cm x 50 μm; 30.2 cm effective length) 15°C +20 kV Injection: 0.1 psi x 5-10 s (1-2 nL) Detection: UV racemic substrates and products at λ = 206 nm

Enzymatic reaction					CE separation		
	Enzyme	Substrate	Inhibitor	Incubation buffer (IB)	Reaction conditions	Background electrolyte (BGE)	CE conditions
[75]	Porcine pancreatic lipase (PL)	DL-Serine methyl ester (DL-SME)	-	200 mM NaHCO ₃ (pH 7.8)	Racemic mixture of DL-SME or DL-TME in IB added to PL	2 M acetic acid + 5 mM chiral crown ether 18C6H4 [(1)-(18-(crown-6)-2,3,11,12-tetracarboxylic acid)]	Uncoated fused-silica capillary 50 cm x 50 µm i.d.; 45 cm effective length
	Wheat germ lipase (WGL)	DL-Threonine methyl ester (DL-TME)			Incubation at 37°C for 2 days Aliquots taken at different time points for CE analysis		Separation voltage: +15 kV Injection: manual at 10 cm elevation for 10 s Detection: C ⁴ D DL-SME, DL-TME, DL-serine and DL-threonine
[80]	Porcine pancreatic lipase (PL)	4-hydroxycoumarin and benzylideneacetone	-	MeOH	PL (immobilized or in-solution) mixed with 1 4-hydroxycoumarin and benzylideneacetone in IB	132.5 mM sodium tetraborate 15 mM SDS (pH 8.5)	Uncoated fused-silica capillary 60 cm x 50 µm i.d.; 50 cm effective length
	immobilized onto 4 metal-organic frameworks (MOFs) or mesoporous silica (SBA-15)				Incubation at 50°C for 1 day Centrifugation at 10K RPM for 5 min to separate the immobilized PL for recycling		Separation voltage: +28 kV Injection: 0.5 psi x 3 s (3 nL) Detection: UV Warfarin, substrates and thiourea at λ = 214 nm

Table 2: CE-based nucleoside kinase assays

Enzymatic reaction					CE separation		
	Enzyme	Substrate	Inhibitor	Incubation buffer (IB)	Reaction conditions	Background electrolyte (BGE)	CE conditions
[91]	Cytosolic 5'-nucleotidase /nucleoside phosphotransferase purified from calf thymus	Inosine	-	50 mM Tris-HCl 20 mM MgCl ₂ 1 mM dithiothreitol (DTT) pH 7.4	<u>Offline reaction:</u> A mixture of: dGMP ATP IB Inosine enzyme Incubation at 37°C for 30 min Aliquots drawn at different time intervals and mixed with cold MeOH to terminate the reaction and stored at -20°C The aliquot was centrifuged at 10000g for 15 min The supernatant was dried and then reconstituted in H ₂ O before CE analysis	50 mM NaH ₂ PO ₄ 40 mM Glycine pH 9.0 adjusted using NaOH	Uncoated fused-silica capillary 50 cm × 50 μm i.d. Temperature: 25°C Separation voltage: +20 kV Injection: 1 psi × 4 s (10 nL) Detection: UV Inosine and dGMP substrates and IMP and deoxyGuanosine products at λ = 254 nm
[92]	Thymidine kinase (TK) Thymidine monophosphate kinase (TMPK)	Thymidine and Thymidine monophosphate (TMP)	-	50 mM Tris-HCl (pH 8)	<u>Offline reaction:</u> Protein extract from insect cell lysate mixed 1:1 (v/v) with reaction solution containing: IB, Thymidine, ATP, MgCl ₂ , Bovine serum albumin, NaF,	20 mM Sodium tetraborate (pH 9.1)	Uncoated fused-silica capillary bubble cell capillary 45.5 cm × 50 μm; 37 cm effective length; 150 μm path length Temperature: 25°C Separation voltage:

Enzymatic reaction					CE separation	
Enzyme	Substrate	Inhibitor	Incubation buffer (IB)	Reaction conditions	Background electrolyte (BGE)	CE conditions
				β-mercaptoethanol.		+23 kV
				Incubation at 37°C for 10 and 20 min The reaction was stopped by boiling for 3 min		Injection: 0.5 psi × 40 s (52 nL)
				Reaction mixture stored at -20°C until CE analyses		Detection: UV thymidine, dTMP and dTDP at λ = 267 nm
[94]	Cellular kinases	Lamivudine	-	The samples were mixed with EDTA, ACN, NaCl and dAMP prior to CE injection		
				Confluent Hep G2 cells incubated at 37°C for 10 h in a medium containing lamivudine.	25 mM Ammonium acetate (pH 10.0)	Uncoated fused-silica capillary 60 cm × 50 μm i.d.
				Cells were lysed by MeOH. The cell lysates were then ultrafiltered then pre-concentrated 100-fold before CE injection.		Separation voltage: +15 kV Injection: Manual at 18 cm elevation for 30 s Detection: ESI-MS Lamivudine and its phosphorylated metabolites Sheath liquid: 100% MeOH at 2 μL min ⁻¹ Negative ionization mode Capillary voltage: -3.6 kV Nebulizing gas flow: 0.41 L min ⁻¹

Enzymatic reaction					CE separation	
Enzyme	Substrate	Inhibitor	Incubation buffer (IB)	Reaction conditions	Background electrolyte (BGE)	CE conditions
[95]	Adenosine kinase (AK) from bovine thymus	<u>Method A</u>	<u>Method A</u>	<u>Method A</u>	<u>Method A (Offline reaction)</u>	<u>Method A</u>
		Adenosine + 7 adenosine nucleoside analogs with different substituents at position 2 of the purine ring	-	20 mM Tris-HCl (pH 7.4)	AK added to the enzyme assay mixture containing: IB MgCl ₂ K ₂ HPO ₄ ATP substrate TMP internal standard	30 mM borate buffer
			<u>Method B & C</u>			100 mM SDS (pH 9.5)
		3 standard AK inhibitors (ABT-702, 5-IT and A-134974)		20 mM Tris-HCl (pH 7.5)		<u>Method B</u>
		<u>Method B & C</u>		20 mM Tris-HCl	Incubation at 37°C for 15 min	20 mM sodium phosphate (pH 7.5)
	Adenosine			0.2 mM MgCl ₂ (pH 7.4)	The reaction was stopped by boiling	<u>Method C</u>
					Aliquots were then injected into CE.	50 mM K ₂ HPO ₄ (pH 6.5)
					<u>Method B (Offline reaction)</u>	
					Similar to method A except: UMP internal standard Inhibitors	<u>Method C</u>
					<u>Method C (Online reaction)</u>	
					1 st plug: IB	
					2 nd plug: diluted AK	
					3 rd plug: Adenosine, ATP, UMP	
						Dry gas flow: 1 L min ⁻¹ <u>Method A & B</u>
						Uncoated fused-silica capillary 40 cm x 75 µm i.d.; 30 cm effective length
						Temperature: 25°C
						Separation current: +95 µA
						Injection (Offline): 0.1 psi x 25 (37.6 nL)
						Detection: UV AMP or nucleoside analogue monophosphate at λ = 260 nm
						Polyacrylamide-coated fused-silica capillary 30 cm x 50 µm i.d.; 20 cm effective length
						Temperature: 37°C
						Separation current: -60 µA

Enzymatic reaction					CE separation	
Enzyme	Substrate	Inhibitor	Incubation buffer (IB)	Reaction conditions	Background electrolyte (BGE)	CE conditions
[97]	Herpes simplex virus-1 (HSV-1) thymidine kinase (TK)	Thymidine Or Acyclovir (ACV) Or Ganciclovir (GCV) Or (E)-5-(2-bromovinyl)-2'-deoxyuridine (BVDU)	Acyclovir (ACV)	50 mM Tris-HCl (pH 7.4)	(internal standard) and inhibitor in IB	Detection: UV AMP at $\lambda = 210$ nm
					4 th plug: IB	
					The reaction was initiated through the application of 5 kV for 12 s	
					Incubation at 37°C for 5 min	
[97]	Herpes simplex virus-1 (HSV-1) thymidine kinase (TK)	Thymidine Or Acyclovir (ACV) Or Ganciclovir (GCV) Or (E)-5-(2-bromovinyl)-2'-deoxyuridine (BVDU)	Acyclovir (ACV)	50 mM Tris-HCl (pH 7.4)	The reaction was stopped by the application of constant current -60 μ A and the analytes were separated	
					The reaction was initiated by adding TK to the reaction mixture previously incubated at 37°C for 2 min containing: IB ACV, GCV or BVDU ATP MgCl ₂ Thymidine (For inhibition assays)	Polyacrylamide-coated fused-silica capillary 30 cm \times 50 μ m OR 75 μ m i.d.; 20 cm effective length
					Incubation at 37°C for 15 min	Temperature:
					The reaction was stopped by boiling for 5 min	Separation current: -60 μ A
[97]	Herpes simplex virus-1 (HSV-1) thymidine kinase (TK)	Thymidine Or Acyclovir (ACV) Or Ganciclovir (GCV) Or (E)-5-(2-bromovinyl)-2'-deoxyuridine (BVDU)	Acyclovir (ACV)	50 mM Tris-HCl (pH 7.4)	The reaction mixtures were transferred to a vial containing UMP or cAMP (internal standard) before CE analysis.	Injection: -6 kV for 30 s
						Detection: UV TMP or monophosphorylated drug analogs at $\lambda = 210$ nm

Enzymatic reaction						CE separation	
	Enzyme	Substrate	Inhibitor	Incubation buffer (IB)	Reaction conditions	Background electrolyte (BGE)	CE conditions
[98]	Human TMPK	dTMP	-	50 mM ammonium acetate (pH 7.0)	TMPK mixed with a range of dTMP concentrations in the presence of: IB, ATP, MgCl ₂ Incubation at 37°C for 5 min The reaction was stopped by boiling for 5 min	80 mM ammonium acetate (pH 9.0)	Uncoated fused-silica capillary (60 cm × 50 μm i.d.; 50 cm effective length) Temperature: 37°C Separation voltage: +15 kV Injection: 0.5 psi × 10 s (12.7 nL) Detection: UV dTMP and dTDP at λ = 254 nm